

Computational Methods in Quantum Field Theory

Kurt Langfeld

School of Mathematics & Statistics, University of Plymouth

Plymouth, PL4 8AA, UK

email: kurt.langfeld@plymouth.ac.uk

November 19, 2007

Abstract

After a brief introduction to the statistical description of data, these lecture notes focus on quantum field theories as they emerge from lattice models in the critical limit. For the simulation of these lattice models, Markov chain Monte-Carlo methods are widely used. We discuss the heat bath and, more modern, cluster algorithms. The Ising model is used as a concrete illustration of important concepts such as correspondence between a theory of branes and quantum field theory or the duality map between strong and weak couplings. The notes then discuss the inclusion of gauge symmetries in lattice models and, in particular, the continuum limit in which quantum Yang-Mills theories arise.

Notes based on a lecture presented at the XIX Physics Graduate Days at the University of Heidelberg, 8th - 12th October 2007.

Contents

1	Statistical data analysis	2
1.1	The central limit theorem	2
1.2	Error analysis	7
1.3	Autocorrelations	10
2	Lessons from the Ising model	12
2.1	Phase transitions	12
2.2	Quantum field theory rising	13
2.3	Mean-field approximation	15
2.4	Duality transformation	17
3	Markov chain Monte-Carlo: the Ising case study	21
3.1	Foundations	21
3.2	Heat-bath algorithm	24
3.3	Cluster update algorithms	26
4	Quantum field theories on computers	28
4.1	Quantum mechanics	28
4.2	Quantum field theory	30
5	Lattice gauge theory	31
5.1	The gauged Ising model	31
5.2	Pure Z_2 gauge theory: 3 and 4 dimensions	33
5.3	Setting up lattice Yang-Mills theory	37
5.4	The fermion doubling problem	41
5.5	Overlap fermions	44
5.6	Measuring observables	45
5.7	The continuum limit	46

1 Statistical data analysis

1.1 The central limit theorem

Assume that we would like to determine a physical observable \bar{x} such as a hadron mass or a decay constant by a numerical calculation involving statistical methods or by a direct experimental measurement. A perfect device would just produce \bar{x} with a single measurement. In practice, such a device does not exist. A realistic device produce a value x in the interval $[x, x + dx]$ with probability $P(x) dx$, where the probability distribution $P(x)$ characterises the apparatus. We will not assume that our experimental device is hampered by systematic errors, but we will assume that the device produces the exact value \bar{x} by an

average over many measurements, i.e.,

$$\int dx x P(x) = \bar{x} , \quad (1)$$

but, depending on $P(x)$, a single measurement can be far from the true value.

As an example, we consider an observable $\bar{x} = 3$ and a crude experiment which can produce any value for between 0 and 6 with equal probability:

$$P(x) = \begin{cases} 1/6 & \text{for } x \in [0, 6] \\ 0 & \text{otherwise.} \end{cases} \quad (2)$$

Obviously, a single measurement for x is not sufficient to reveal the true observable. The only thing we can do is to repeat the measurement n times and to consider the average:

$$y = \frac{1}{n} [x_1 + \dots + x_n] ,$$

where x_1 to x_n are the values obtained from each of the measurements. For the moment, we will assume that the measurements are *independent*, i.e., that the probability for finding a set $\{x_1 \dots x_n\}$ of data is given by:

$$P(x_1, \dots, x_n) = P(x_1) \dots P(x_n) .$$

The crucial question is to which accuracy have we estimated the true observable \bar{x} ?

The answer can be inferred from the probability distribution $Q(y)$ for the value y :

$$Q_n(y) = \int \prod_{i=1}^n dx_i \delta \left(y - \frac{1}{n} [x_1 + \dots + x_n] \right) P(x_1) \dots P(x_n) . \quad (3)$$

Given the proper normalisation of the single event distributions, i.e.,

$$\int dx_i P(x_i) = 1 ,$$

using (1), we can easily show that the average of y coincides with the observable:

$$\begin{aligned} \bar{y} &= \int dy y Q_n(y) \\ &= \int dy \int \prod_{i=1}^n dx_i \frac{1}{n} [x_1 + \dots + x_n] \delta \left(y - \frac{1}{n} [x_1 + \dots + x_n] \right) P(x_1) \dots P(x_n) . \\ &= \int \prod_{i=1}^n dx_i \frac{1}{n} [x_1 + \dots + x_n] P(x_1) \dots P(x_n) = \frac{1}{n} n \int dx x P(x) = \bar{x} . \end{aligned}$$

A natural measure for the error σ of our estimate is provided by the second moment:

$$\sigma^2(n) = \int dy (y - \bar{y})^2 Q_n(y), \quad (\text{the variance}). \quad (4)$$

If the distribution $Q_n(y)$ peaks around the true value for our observable \bar{x} and $\sigma(n)$ is tiny, it would mean that a single estimator y has high probability to fall close to \bar{x} with high probability implying that it yields a good approximation to \bar{x} .

Let us study the moments of the distribution $Q(y)$:

$$q_m = \int dy Q_n(y) y^m. \quad (5)$$

In order to draw further conclusions, we need to restrict the classes of single event probability distributions $P(x)$: we will assume that its Fourier transform

$$\bar{P}(\beta) = \int dx P(x) \exp\{-i\beta x\} \quad (6)$$

is an analytic function of β at $\beta = 0$. As a consequence, the moments of $P(x)$ exist and are given by:

$$p_m = \int dx P(x) x^m = i^m \frac{d^m}{d\beta^m} \bar{P}(\beta) |_{\beta=0}. \quad (7)$$

We will further assume that $\bar{P}(\beta)$ vanishes for $|\beta| \rightarrow \pm\infty$. This seems to be quite a weak constraint. I point out, however, that systems with rare but large fluctuations generically fail to possess higher moments. One example is stock market indices [1].

Our aim is to express the moments of $Q_n(y)$ in terms of the moments of $P(x)$. For this purpose, we rewrite the δ -function in (3) as

$$\delta\left(y - \frac{1}{n} [x_1 + \dots + x_n]\right) = \int \frac{d\alpha}{2\pi} \exp[i\alpha y] \prod_{i=1}^n \exp\left\{-i\frac{\alpha}{n} x_i\right\}, \quad (8)$$

and find

$$Q_n(y) = \int \frac{d\alpha}{2\pi} \exp(i\alpha y) \left[\int dx P(x) \exp\left\{-i\frac{\alpha}{n} x\right\} \right]^n, \quad (9)$$

$$= \int \frac{d\alpha}{2\pi} \exp(i\alpha y) \left[\bar{P}\left(\frac{\alpha}{n}\right) \right]^n. \quad (10)$$

The moments of $Q_n(y)$ are then obtained from

$$q_m = \int dy \int \frac{d\alpha}{2\pi} (-i)^m \frac{d^m}{d\alpha^m} \left[\exp(i\alpha y) \right] \bar{P}^n\left(\frac{\alpha}{n}\right). \quad (11)$$

After a series of partial integrations with respect to α (note that boundary terms vanish by virtue of our above assumptions), the latter equation is given by

$$\begin{aligned} q_m &= \int dy \int \frac{d\alpha}{2\pi} \exp(i\alpha y) (i)^m \frac{d^m}{d\alpha^m} \left[\bar{P}^n \left(\frac{\alpha}{n} \right) \right] \\ &= \int \frac{d\alpha}{2\pi} \frac{1}{n^m} \int dy \exp(i\alpha y) (i)^m \frac{d^m}{d\beta^m} \left[\bar{P}^n(\beta) \right] = \frac{i^m}{n^m} \frac{d^m}{d\beta^m} \left[\bar{P}^n(\beta) \right] \Big|_{\beta=0}. \end{aligned} \quad (12)$$

Of particular interest are the so-called cumulants $c_k[Q_n]$ of the distribution $Q_n(y)$. These are defined via the generating function

$$T_Q(x) = \sum_{m=0}^{\infty} \frac{1}{m!} q_m x^m, \quad c_k[Q_n] := \frac{d^k}{dx^k} \ln T_Q(x) \Big|_{x=0}. \quad (13)$$

Note that in particular we find for the 'error' σ in (4)

$$\sigma^2 = q_2 - q_1^2 = c_2[Q_n]. \quad (14)$$

Using Taylor's theorem and the explicit expression (12), we find

$$T_Q(x) = \bar{P}^n \left(\frac{ix}{n} \right), \quad c_k[Q_n] = \frac{i^k}{n^{k-1}} \left[\ln \bar{P}(0) \right]^{(k)}, \quad (15)$$

where (k) denotes the k th derivative. Introducing the cumulants $c_k[P]$ of the single event distribution as well, i.e.,

$$c_k[P] = i^k \left[\ln \bar{P}(0) \right]^{(k)}, \quad (16)$$

we arrive at a very important result:

$$c_k[Q_n] = \frac{1}{n^{k-1}} c_k[P]. \quad (17)$$

Note that the cumulants $c_k[P]$ are finite numbers which characterise the single event probability distribution. Equation (17) then implies that for increasing number of measurements n , the higher ($k > 1$) cumulants of $Q_n(y)$ vanish. In particular, we find that

$$\sigma(n) = \sqrt{c_2[Q_n]} = \frac{\sqrt{c_2[P]}}{\sqrt{n}} \propto 1/\sqrt{n}. \quad (18)$$

For the above example, we find

$$p_1 = \frac{1}{6} \int_0^6 dx x = 3, \quad p_2 = \frac{1}{6} \int_0^6 dx x^2 = 12, \quad c_2[P] = 12 - 3^2 = 3, \quad (19)$$

and therefore

$$\sigma(n) = \sqrt{3/n}.$$

It is well known that if $c_k[G] = 0$ for $k > 2$, the probability distribution G is a Gaussian. We therefore expect that if n is chosen sufficiently large so that we can neglect $c_k[Q_n]$ with $k > 2$, we should be able to approximate $Q_n(y)$ by a Gaussian. To support this claim (without mathematical rigour), we start from (10):

$$Q_n(y) = \int \frac{d\alpha}{2\pi} \exp(i\alpha y) \exp \left\{ n \ln \left[\bar{P} \left(\frac{\alpha}{n} \right) \right] \right\} ,$$

and expand the logarithm with respect to α :

$$\begin{aligned} Q_n(y) &= \int \frac{d\alpha}{2\pi} \exp(i\alpha y) \exp \left\{ n \sum_{k=0}^{\infty} \frac{1}{k!} [\ln \bar{P}(0)]^{(k)} \left(\frac{\alpha}{n} \right)^k \right\} \\ &= \int \frac{d\alpha}{2\pi} \exp(i\alpha y) \exp \left\{ n \sum_{k=1}^{\infty} \frac{1}{k!} c_k[P] \left(-i \frac{\alpha}{n} \right)^k \right\} , \end{aligned}$$

where we have used $\bar{P}(0) = \int dx P(x) = 1$ and the definition of the cumulants of P in (16). Using $c_1[P] = p_1 = \bar{x} = \bar{y}$, we find:

$$Q_n(y) = \int \frac{d\alpha}{2\pi} \exp[i\alpha(y - \bar{y})] \exp \left\{ -\frac{1}{2} c_2[P] \left(\frac{\alpha^2}{n} \right) + \mathcal{O}(\alpha^3/n^2) \right\} \quad (20)$$

Note that the dominant contributions from the α integration arises from the regime where $\alpha < \sqrt{n}$. In this regime, the correction term is of order

$$\mathcal{O}(\alpha^3/n^2) \approx \mathcal{O}(1/\sqrt{n})$$

and will be neglected for sufficiently large n . The remaining integral can be easily performed:

$$Q_n(y) \approx \frac{1}{\sqrt{2\pi} \sigma} \exp \left\{ -\frac{(y - \bar{y})^2}{2\sigma^2} \right\} , \quad \sigma^2 = \frac{c_2[P]}{n} . \quad (21)$$

which is the celebrated Gaussian distribution. This finding is called the *central limit theorem*: if the moments of probability distribution $P(x)$ exist, the probability distribution for the average y can be approximated by a Gaussian for sufficiently large n given that the standard deviation σ is properly scaled with n .

Let us discuss this result. Figure 1 shows the distributions $Q_n(y)$ for $n = 1, 2, 3$ and $n = 10$. Already for $n = 10$ the distribution is well approximated by the Gaussian.

The existence of at least the moment $c_2[P]$ of the single event distribution is crucial for the error reduction by repeated measurements. Let us consider a Lorentz distribution for the moment:

$$P_L(x) = \frac{1}{\pi b} \frac{1}{1 + (x/b)^2} . \quad (22)$$

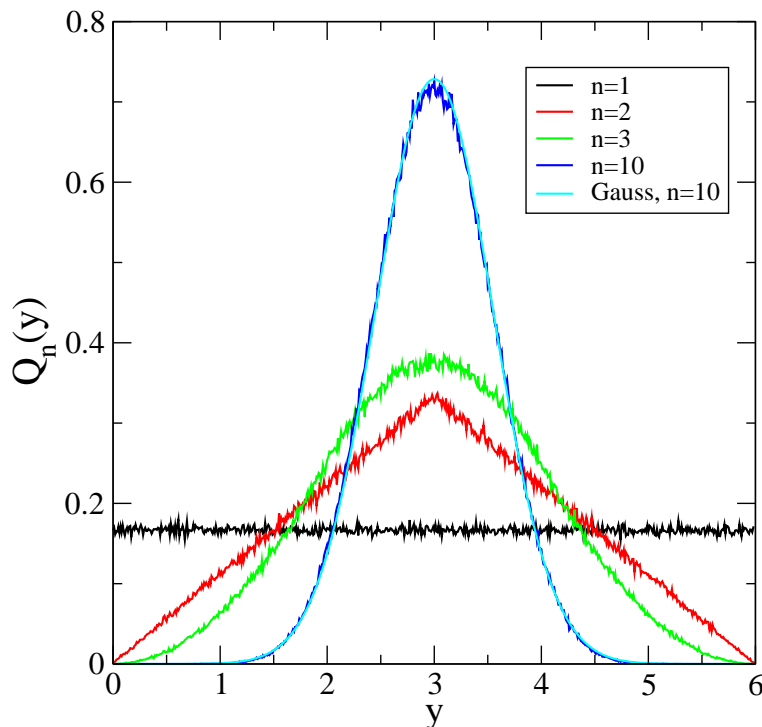


Figure 1: Illustration of the central limit theorem: probability distributions of the average y after n measurements.

With the naked eye this distribution resembles the Gaussian. The crucial difference is, however, that the second moment does not exist:

$$\int dx x^2 P_L(x) \longrightarrow \infty .$$

The Fourier transform of $P_L(x)$ does, however, exist

$$\bar{P}_L(\beta) = \exp\left\{-b|\beta|\right\} . \quad (23)$$

If we now repeat the measurements n times, the distribution of the average y is, according to (10), by

$$Q_n(y) = \int \frac{d\alpha}{2\pi} \exp(i\alpha y) \left[\exp\left(-b\frac{\alpha}{n}\right) \right]^n = P_L(y) .$$

Obviously, the probability distribution does not change at all even if we repeat the measurements many times. This actually implies that it is impossible to experimentally gain a reliable value for the observable \bar{x} .

1.2 Error analysis

Let us return to the example in (2), and let us assume a group of experimentalists has performed $n = 12$ measurements with the result:

2.813	2.021	0.331	0.865
5.394	5.937	5.027	1.556
0.325	2.750	1.283	3.890

The average over these values and an estimate $\langle x^2 \rangle$ of $c_2[P]$ are given by

$$y = \frac{1}{n} \sum_{k=1}^n x_k \approx 2.683, \quad \langle x^2 \rangle = \frac{1}{n} \sum_{k=1}^n x_k^2 \approx 3.581. \quad (24)$$

We point out that 3.581 is a poor estimate of the true value (19) of $c_2[P] = 3$, but it gives the order of magnitude. With this estimate for $c_2[P]$, we find for the error (18)

$$\sigma(n = 12) \approx \sqrt{\frac{3.581}{12}} \approx 0.546.$$

Hence, the final 'experimental' result for the observable would be

$$\bar{x} \approx 2.683 \pm 0.546 = 2.7(5). \quad (25)$$

Note that the true result $\bar{x} = 3$ lies well with the reach of the error bars.

The above experiment was repeated by several research labs. Depending on the budget and the focus of research, different labs produce different numbers n of measurements:

	CERN	GSI	DESY	BNL
n	120	50	78	150
y	3.112 ± 0.163	2.764 ± 0.255	3.110 ± 0.207	3.083 ± 0.143

The smallest error was produced by the largest experiment (BNL). We could just quote their result, but it would be a pity to disregard a total of 248 measurements which were carried out by the other groups. How can we obtain a 'world average' for the observable \bar{x} and how can we quantify its (statistical) error?

To answer these questions, we assume that the number n of each measurement was large enough to approximate the distribution of an individual result y_k , $k = 1 \dots N$ (where $N = 4$ for the above example) by a Gaussian (21):

$$Q(y_l) \approx \frac{1}{\sqrt{2\pi} \sigma_l} \exp \left\{ -\frac{(y_l - \bar{x})^2}{2\sigma_l^2} \right\}. \quad (26)$$

For the world average y we make the ansatz

$$y = \sum_{l=1}^N a_l y_l, \quad \sum_{l=1}^N a_l = 1. \quad (27)$$

The weights a_l must be chosen in an optimal way. This choice will depend on the errors σ_l of the individual experiments. In particular, the experiment with the smallest error should contribute to the world average with the largest weight. Assuming that the experiments at the different labs were carried out independently, the probability distribution of the world average is now given by

$$W(y) = \int \prod_{k=1}^N dy_k \delta\left(y - \sum_{l=1}^N a_l y_l\right) Q(y_1) \dots Q(y_N) . \quad (28)$$

Representing the δ -function in terms of a Fourier integral over α (see (8)), the integrations over $y_1 \dots y_N$ can be easily performed:

$$W(y) = \int \frac{d\alpha}{2\pi} \exp\{i(y - \bar{x})\alpha\} \exp\left\{-\frac{\alpha^2}{2} \sum_l a_l^2 \sigma_l^2\right\} .$$

Performing the α integration finally yields:

$$Q(y) \approx \frac{1}{\sqrt{2\pi} \sigma} \exp\left\{-\frac{(y - \bar{x})^2}{2\sigma^2}\right\} , \quad \sigma^2 = \sum_l a_l^2 \sigma_l^2 . \quad (29)$$

The optimal result is achieved if the error squared, i.e., σ^2 , is as small as possible. Here, we must take into account the normalisation condition in (27). We therefore minimise

$$\sum_l \left[a_l^2 \sigma_l^2 - \lambda a_l \right] \longrightarrow \min , \quad (30)$$

where λ is a Lagrange multiplier. The global minimum is easily obtained:

$$a_l = \frac{\lambda}{2\sigma_l^2} , \quad \frac{2}{\lambda} = \sum_l \frac{1}{\sigma_l^2} . \quad (31)$$

The minimal value for σ^2 then satisfies

$$\sigma^2 = \frac{\lambda}{2} \quad \Rightarrow \quad \frac{1}{\sigma^2} = \sum_l \frac{1}{\sigma_l^2} . \quad (32)$$

The optimal choice for the weights can therefore also be written as

$$a_l = \frac{\sigma^2}{\sigma_l^2} . \quad (33)$$

Let us return to the above example. We find

$$\begin{aligned} \sigma &\approx 0.089 , \\ a_1 &\approx 0.30 , \quad a_2 \approx 0.12 , \quad a_3 \approx 0.19 , \quad a_4 \approx 0.39 . \end{aligned} \quad (34)$$

With the weights at our disposal, we easily find the optimal value for the world average $y \approx 3.059$. Together with the error in (34), the final result is

$$\bar{x} = 3.059 \pm 0.089 = 3.06(9) . \quad (35)$$

Note that the true result $\bar{x} = 3$ is again covered within error bars and that the error became significantly smaller than that of the best result provided by the BNL group.

1.3 Autocorrelations

In the previous subsections, we have repeatedly assumed that the measurements x_i are independent. We will see below that a vital tool of computational quantum field theory is to use information from the measurement x_i to obtain the value for x_{i+1} . In this case, the data set $x_i, i = 1 \dots n$ is generated by the chain

$$x_1 \rightarrow x_2 \rightarrow \dots \rightarrow x_{n-1} \rightarrow x_n,$$

and the probability of finding a particular set does not factorise anymore:

$$P(x_1, \dots, x_n) \neq P(x_1) \dots P(x_n).$$

In the context of QFT simulations we will, however, make an effort to render the values x_i as independent as possible. This generically implies that events which are separated by some ‘time’ τ , i.e., the events x_i and $x_{i+\tau}$, can be considered as statistically independent. The trick for obtaining an idea of the error of the estimator is to group b measurements together:

$$y_\nu = \frac{1}{b} \sum_{i=1}^b x_{\nu+i}, \quad \nu = 1 \dots M, \quad M = \frac{n}{b}, \quad (36)$$

where we choose

$$1 \leq \tau \ll b. \quad (37)$$

This latter constraint implies that the values y_ν are statistically independent and that they have a Gaussian distribution because of the central limit theorem. The quantities of interest are the average

$$\bar{y} = \frac{1}{M} \sum_{\nu=1}^M y_\nu, \quad (38)$$

which converges to the observable \bar{x} in the limit $M \rightarrow \infty$, and the corresponding error

$$\sigma^2 = \frac{1}{M} c_2[P_y] = \frac{b}{n} c_2[P_y]. \quad (39)$$

where the cumulant $c_2[P_y]$ is given by

$$c_2[P_y] = \left\langle \frac{1}{M} \sum_{\nu=1}^M y_\nu^2 \right\rangle - \left[\left\langle \frac{1}{M} \sum_{\nu=1}^M y_\nu \right\rangle \right]^2, \quad (40)$$

with

$$\langle f \rangle = \int \prod_{l=1}^n dx_l f(x_1 \dots x_n) P(x_1, \dots, x_n).$$

Assuming translational invariance, i.e.,

$$\langle x_{\nu+i} x_{\nu+k} \rangle = \langle x_i x_k \rangle,$$

we find

$$c_2[P_y] = \frac{1}{b^2} \sum_{i=1}^b \sum_{k=1}^b c(k-i), \quad c(k-i) = \langle x_i x_k \rangle - \langle x_i \rangle \langle x_k \rangle, \quad (41)$$

where $c(k-i)$ is called the *autocorrelation function*. Introducing the relative distance $t = k - i$, and trading the summation over k in (41) for a summation over t , we find

$$c_2[P_y] = \frac{1}{b^2} \sum_{i=1}^b \sum_{t=1-i}^{b-i} c(t). \quad (42)$$

Interchanging the summation indices t and i and after summing over i , this last equation becomes:

$$c_2[P_y] = \frac{1}{b} c(0) + \frac{2}{b^2} \sum_{t=1}^{b-1} (b-t) c(t).$$

We have already mentioned that the measurements x_i and $x_{i+\tau}$ are (almost) uncorrelated. The equivalent statement is that the correlation function vanishes for sufficiently large arguments:

$$c(t) \approx 0, \quad \text{for } t > \tau.$$

For $b \gg \tau$, we approximately find:

$$c_2[P_y] \approx \frac{1}{b} c(0) + \frac{2}{b^2} \sum_{t=1}^{b-1} b c(t) = \frac{1}{b} \sum_{t=1-b}^{b-1} c(t). \quad (43)$$

It is convenient to introduce the *normalised autocorrelation function* by

$$\rho(t) = \frac{c(t)}{c(0)}, \quad c(0) = \langle x^2 \rangle - \langle x \rangle^2 = c_2[P_x]. \quad (44)$$

The *integrated autocorrelation time* is then defined by

$$\tau = \frac{1}{2} \sum_{t=1-b}^{b-1} \rho(t) = \frac{1}{2} + \sum_{t=1}^{b-1} \rho(t). \quad (45)$$

Inserting (45,44,43) into (39), we finally obtain for the error which should be attributed to our estimate \bar{y} in (38):

$$\sigma^2 = \frac{2\tau}{n} c_2[P_x]. \quad (46)$$

Let us perform a consistency check by considering the special case that the measurements are uncorrelated. In this case, the autocorrelation function $\rho(t)$ vanishes for $t \geq 1$, and the autocorrelation time is given by $\tau = 1/2$. We indeed recover the familiar result

$$\sigma^2 = \frac{1}{n} c_2[P_x], \quad \text{for independent measurements.} \quad (47)$$

Note that autocorrelations increase the error bars. Not knowing the autocorrelations in a numerical simulations leads us to the erroneous assumption that the error of the estimator is given by (47), while the true result is by a factor τ larger. Not knowing the autocorrelations always leads to an underestimation of the statistical error.

2 Lessons from the Ising model

2.1 Phase transitions

A phase transition occurs if the properties of matter change qualitatively when an external parameter, such as temperature, is altered. The phase transition of water from a liquid to a gas phase when the temperature exceeds roughly $\approx 100^0$ Celsius (under normal conditions), is well known from everyday life. A second example is the ferromagnet: the interaction between microscopic spins favour a unique orientation of the spins. This yields an *ordered phase* at low temperatures. Above the critical temperature, called the *Curie temperature* in the present context, the spins are organised in a *disordered phase*.

Let us assume that a ferromagnet is in the disordered phase at a temperature slightly bigger than the critical temperature T_c . If we decrease the temperature, the information of the unique orientation spreads over the spin lattice. This ‘Gedankenexperiment’ shows that the spatial correlation of the spins becomes large at the critical temperature. This phenomenon, is quantified with the help of the spin-spin *correlation function*:

$$\left\langle \sigma(x) \sigma(y) \right\rangle \propto \exp \left\{ -\frac{|x-y|}{\xi} \right\}. \quad (48)$$

The *correlation length* ξ obviously measures the spatial distance over which the spins show roughly the same orientation. Close to the phase transition, i.e. for $T \gtrsim T_c$, ξ becomes large anticipating the ordered phase:

$$\xi \approx \xi_+ \left| 1 - \frac{T}{T_c} \right|^{-\nu}, \quad (T \gtrsim T_c), \quad (49)$$

where ν is a positive number. The divergence of the correlation length at the phase transition is characteristic for a transition of *2nd* (or higher) order. In the case of a *1st order* transition, the increase of ξ is hindered by the nucleation of bubbles which contain chunks of the new state of matter. These bubbles provide additional disorder and the correlation length stays finite.

For phase transitions above first order, the singularity of the correlation length has its fingerprint in many other thermodynamical quantities such as the *specific heat* C or the *magnetic susceptibility* χ :

$$C \approx C_0 \left| 1 - \frac{T}{T_c} \right|^{-\alpha}, \quad \chi \approx \chi_0 \left| 1 - \frac{T}{T_c} \right|^{-\gamma}, \quad (T \gtrsim T_c).$$

The *critical exponents* ν , α , γ are independent of the microscopic properties of the spin model (such as the lattice geometry), and only depend on the symmetries (present at the transition) and the number of dimensions. They are often used to sort solid state physics models into the so-called *universality classes*.

2.2 Quantum field theory rising

Let the *lattice spacing* a denote the distance between two neighbouring lattice sites. In the previous subsection, we found that the correlation length diverges if the coupling constant β (or inverse temperature in the present context, $\beta = 1/T$) approaches its critical value (see (49)). This statement can be phrased in units of the lattice spacing as

$$\frac{\xi}{a} = \kappa \left(\beta_c - \beta \right)^{-\nu}, \quad \beta \lesssim \beta_c, \quad (50)$$

where κ is a dimensionless constant which can be obtained by numerical means.

Let us now reinterpret these findings. Rather than saying that ξ diverges and a is fixed, we say that the correlation length ξ is fixed and is given by an observable in physical units. We will see that this interpretation of the same data defines a **quantum field theory**. For fixed correlation length ξ , (50) defines the lattice spacing as a function of β , i.e., $a \rightarrow a(\beta)$,

$$a(\beta) = \frac{1}{\kappa} (\beta - \beta_c)^\nu \xi, \quad \beta \rightarrow \beta_c. \quad (51)$$

The key point is if we make the number of spins bigger and bigger and, at the same time, the distance a between the spins smaller and smaller, we will obtain a field theory in the limit $a \rightarrow 0$. For the 2d Ising model on a cubic lattice, we have $\beta_c \approx 0.44$ and $\nu = 1$. The field theory limit is then approached when a vanishes linearly with $\beta - \beta_c$:

$$a(\beta) = \frac{\xi}{\kappa} (\beta - \beta_c), \quad (2d \text{ Ising model}).$$

Note that the dimensionless parameter β is not at our disposal anymore, since it specifies the magnitude of the lattice spacing. Instead, the value of ξ parameterises the emerging quantum field theory. The exchange of a dimensionless parameter for a scale dependent one in a quantum field theory is known as *dimensional transmutation*. It is a generic feature of quantum field theories. For instance in the case of perturbative QCD, the dimensionless gauge coupling g is eliminated in favour of the scale dependent parameter Λ_{QCD} .

Let us assume that a certain correlation function was obtained by a numerical simulation of a classical lattice model for large values $|x - y|$,

$$D(|x - y|) = \left\langle F(\phi(x)) F(\phi(y)) \right\rangle \propto \exp\left\{-m|x - y|\right\}, \quad (52)$$

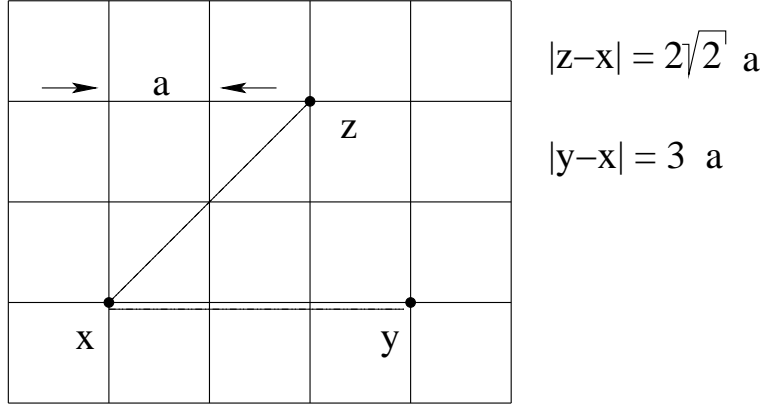


Figure 2: Spin correlation along the diagonal and the symmetry axis, respectively.

where m is called the **screening mass**. Since the distance $|x - y|$ is only known in units of the lattice spacing by construction, the simulation will provide the mass in units of the lattice spacing as a function of β , i.e. $ma(\beta)$. If universality holds, one finds the characteristic scaling of the lattice model, i.e.,

$$ma(\beta) = \kappa_m \left(\beta_c - \beta \right)^\nu, \quad \beta \lesssim \beta_c. \quad (53)$$

Using (50), we see that the product $m\xi$ approaches a constant in the vicinity of the critical limit:

$$m\xi = ma \frac{\xi}{a} = \kappa_m \kappa. \quad (54)$$

Note that κ and κ_m are two c-numbers which we obtain from the numerical simulations. With the help of these two numbers we can “measure” the desired mass m in units of $1/\xi$, where ξ is the only free parameter of our theory.

In the case of a quantum field theory, we expect that due to the isotropy of the vacuum the correlation function (52) only depends on the distance between x and y . In the classical lattice model, continuous rotational symmetry is violated due to the presence of the cubic lattice, and it might happen that the quantum field theory which emerges from the lattice model inherits the anisotropy. This anisotropy can be measured by comparing the correlation length in lattice units along a lattice symmetry axis, ξ , and along the diagonal direction, ξ_d (see figure 2). As far as global symmetries are concerned, the symmetry under consideration is restored in the critical limit (51):

$$\xi_d = \xi, \quad \text{for } a \rightarrow 0.$$

Further details on the restoration of rotational symmetry in the context of the 2-dimensional Ising model can be found in [2].

2.3 Mean-field approximation

The starting point for a thermodynamical description of the Ising model is the partition function:

$$\mathcal{Z} = \sum_{\{\sigma_x\}} \exp(-\beta H(\sigma)) \quad (55)$$

where $\beta = 1/T$ and where a *spin* $\sigma_x = \pm 1$ is associated with each site x of the square lattice. The sum in (55) extends over all possible spin configurations. The *ferromagnetic* interaction favours a unique orientation of the spins, and is described by

$$H(\sigma) = - \sum_{\langle xy \rangle} \sigma_x \sigma_y , \quad (56)$$

where the sum extends over all pairs $\langle xy \rangle$ of nearest neighbours. In order to preserve translational invariance, periodic boundary conditions are often used in particle physics applications, although these conditions are difficult to interpret in the solid state physics context.

In order to gain an initial insight into the phase structure of the Ising model, we choose a particular spin σ_{x_0} of the lattice, and assume heuristically that that we might replace the neighbouring spins by the mean

$$\langle \sigma \rangle = \frac{1}{\mathcal{Z}} \sum_{\{\sigma_x\}} \sigma_{x_0} \exp(-\beta H(\sigma)) . \quad (57)$$

The Hamiltonian is then approximately given by

$$H(\sigma_{x_0}) \approx \text{const.} - 4\langle \sigma \rangle \sigma_{x_0} . \quad (58)$$

Note that each spin possesses 4 neighbours on a cubic 2d square lattice. Equation (57) turns into a self-consistency equation to determine the $\langle \sigma \rangle$, which can be interpreted as the magnetisation per site:

$$\langle \sigma \rangle = \frac{1}{\mathcal{N}} \sum_{\sigma_{x_0}=\pm 1} \sigma_{x_0} \exp(-\beta H(\sigma)) , \quad (59)$$

$$\mathcal{N} = \sum_{\sigma_{x_0}=\pm 1} \exp(-\beta H(\sigma)) . \quad (60)$$

Performing the sum over σ_{x_0} leaves us with a non-linear equation:

$$\langle \sigma \rangle = \tanh(4\beta \langle \sigma \rangle) . \quad (61)$$

Before we proceed with a numerical solution of this equation, we point out that (61) always possesses the trivial solution

$$\langle \sigma \rangle = 0 .$$

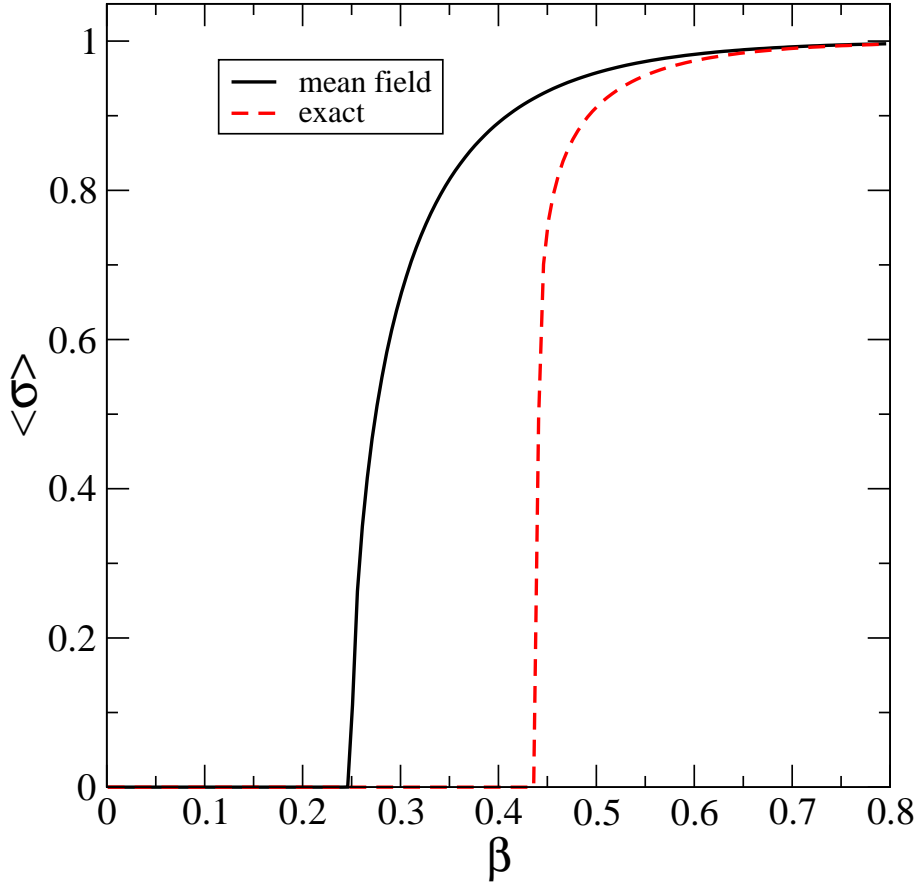


Figure 3: Magnetisation per site as function of the inverse temperature β ; solid line: mean field approximation; dashed line: exact

A graphical inspection of (61) easily shows that for

$$\beta > \frac{1}{4}, \quad (62)$$

two non-trivial solutions $\pm c$, for $c > 0$ exist. The physical interpretation of the solution is clear: for sufficiently small temperature (high β), an ordered phase exists. The critical value is, in mean-field approximation, given by

$$\beta_c^{\text{MF}} = 1/4. \quad (63)$$

Equation (61) can be easily solved numerically with the Newton method or by fixed point iteration. The result for the magnetisation as a function of the inverse temperature is shown in figure 3. Also shown is the exact result [3,4]:

$$\langle \sigma \rangle = \left[1 - \frac{1}{\sinh^4(2\beta)} \right]^{1/8} \quad (64)$$

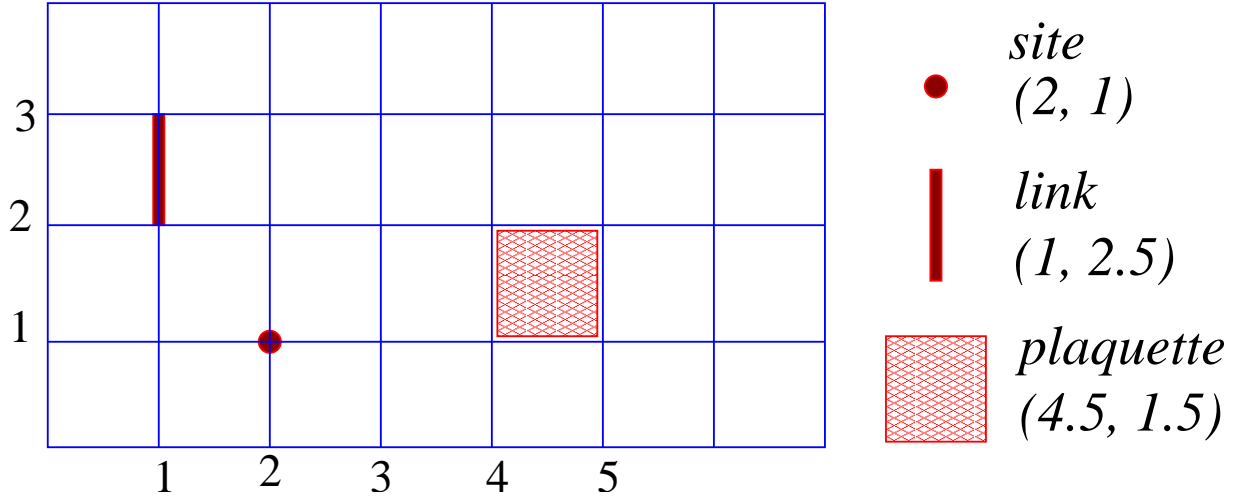


Figure 4: Geometrical objects on a lattice.

The mean-field result qualitatively reproduces the correct phase structure. The mean field approximation is able to describe the transition from the disordered to the ordered phase. However, the mean field approximation fails at a quantitative level. The correct value for the critical value, which was already obtained by Kramers and Wannier in 1941 [3], is given by

$$\beta_c = 0.44068679\dots \quad (65)$$

is significantly underestimated. Also the rise of the magnetisation close to β_c is not correctly reproduced. A Taylor expansion of (61) with respect to β around $\beta_c^{\text{MF}} = 1/4$ (and therefore also with respect to σ), yields:

$$\langle \sigma \rangle \approx \sqrt{12} \left(\beta - \beta_c \right)^b, \quad b = \frac{1}{2}. \quad (66)$$

The mean field critical exponent of 1/2 is much too large compared with the exact exponent of $b_{\text{exact}} = 1/8$.

The advantage of the mean-field approximation is that it can be easily applied to a variety of models (e.g. the Ising model in $d > 2$ where no exact results are available). It often provides a correct first impression of the phase structure. The disadvantage is that it is difficult to improve the approximation in a systematic way.

2.4 Duality transformation

Let us list different geometrical objects on a lattice. The *sites* on a lattice are labelled by integer coordinates. *Links* are short line segments which join two neighbouring sites on the lattice. In order to unambiguously address a link on the lattice, we use coordinates which are integers with the exception of one coordinate which is half integer, such as 2.5 (see figure 4 for an illustration). Another important object is the so-called *plaquette*,

which is an elementary square of the cubic lattice. Two coordinates are half integer when a plaquette is addressed. In higher dimensions, there are also *cubes*, and their coordinates are half integer, while the other coordinates are integer.

The *dual lattice* is an important object which helps to gain non-perturbative information for certain lattice models. The coordinates of the dual lattice are obtained by adding 0.5 to all coordinates of the lattice. If we consider a d dimensional lattice model, the duality transformation maps an x -dimensional geometrical object into a $d - x$ dimensional object on the dual lattice. Let us consider 2 dimensions. A site, such as (2, 4) is mapped into (2.5, 4.5), which are the coordinates of a plaquette, while a link, e.g. (1.5, 5), maps into another link namely (2, 5.5).

With these prerequisites, let us consider the probabilistic measure of the 2d Ising model. Since the product $\sigma_x \sigma_y$ can only be ± 1 , we expand:

$$\exp\{\beta \sigma_x \sigma_y\} = a + b \sigma_x \sigma_y .$$

Inserting both possible values for the product $\sigma_x \sigma_y$, we find:

$$a + b = e^\beta , \quad a - b = e^{-\beta} ,$$

and finally:

$$\exp\{\beta \sigma_x \sigma_y\} = \cosh \beta + \sinh \beta \sigma_x \sigma_y . \quad (67)$$

Hence, the partition function in (55) can be written as

$$\mathcal{Z} = \sum_{\{\sigma_x\}} \cosh^{2N} \prod_{\langle xy \rangle} [1 + \tanh \beta \sigma_x \sigma_y] . \quad (68)$$

where x and y are nearest neighbours on the lattice, and the corresponding link is denoted by $\langle xy \rangle$. Note also that, in 2 dimensions, there are $2N$ links for a lattice with N sites. In order to perform the sum over all spin configurations in (68), we use the important relations:

$$\sum_{\sigma=\pm 1} \sigma = 0 , \quad \sum_{\sigma=\pm 1} \sigma^2 = 2 .$$

Hence, if we perform the sum over the spin σ_x in (68), we must make sure that it appears twice (or an even number of times) when we expand the products of the square brackets.

Thus, if we avoid a vanishing contribution to the partition function, integration over the spins generates closed loops the corners of which are marked by a pair of spins. For each link of the closed loop, we get a factor $\tanh \beta$. Hence, after we have integrated out all spins, the partition function can be written as:

$$\mathcal{Z} = \cosh^{2N} \beta 2^N \sum_{\text{loops}} [\tanh \beta]^{N(L)} , \quad (69)$$

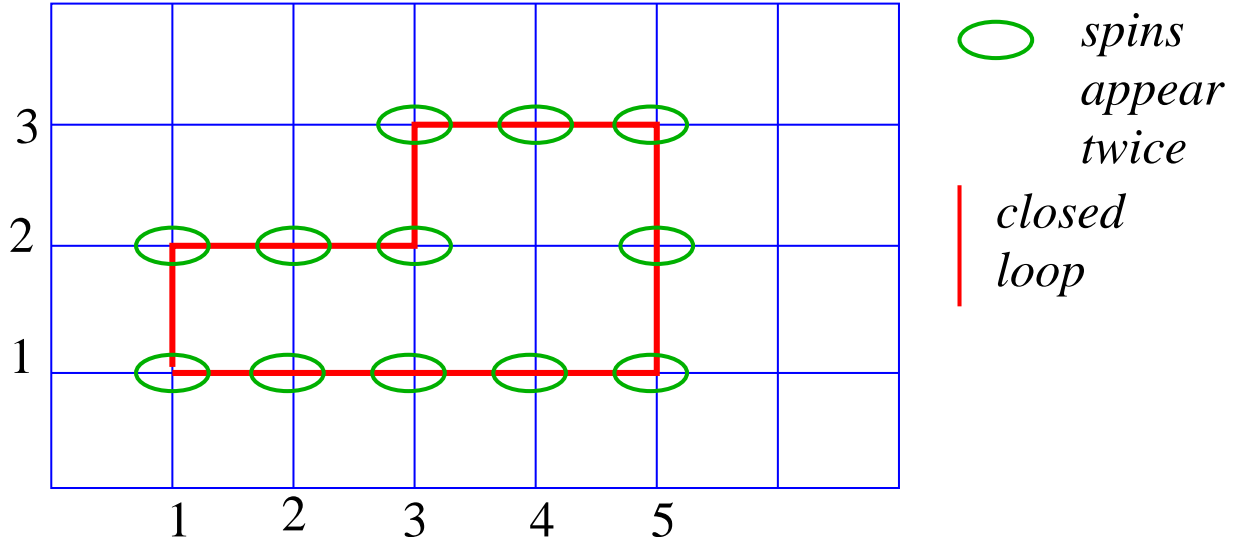


Figure 5: Integration over spins generate closed loops.

where $N(L)$ is the number of links of the closed loop L . Note that we obtained a factor of 2 for each sum over a particular spin σ . This gives rise to the prefactor 2^N in front of the sum in (69). We now have converted the Ising model into a string theory, but we have not gained much information on the Ising model so far. To proceed further, we must control the sum over closed loops. For this purpose, we introduce new variables $\tau = \pm 1$ which are associated with the plaquettes (see figure 6). If we consider two neighbouring plaquettes, there is always just one link between them. Now we say that if the product of the two neighbouring plaquettes is -1 , the corresponding link is part of the loop. If the product is 1, the link is not part of the loop. The advantage of the τ variables is that we can randomly assign ± 1 to them and all loops which we produce are closed. Hence, summing over all possible τ configurations will do the sum over all possible closed loops for us.

Note that each plaquette of the lattice is mapped to a site on the dual lattice. The link between two neighbouring plaquettes is mapped into the link between the adjacent sites of the dual lattice. Finally, we must express $N(L)$ in terms of the τ variables. For this purpose, we have to count all *activated* links (links which are part of a loop) on the lattice. It is easy to check that

$$N(L) = \sum_{\langle x_d y_d \rangle} \frac{1}{2} \left[1 - \tau_{x_d} \tau_{y_d} \right] \quad (70)$$

counts these links: if two neighbouring τ s are equal, they do not contribute to $N(L)$, and if they are different, they contribute 1 as they should. Using the τ -representation of the closed loops, the partition function (69) becomes

$$\mathcal{Z} = [\cosh \beta]^{2N} [2 \tanh \beta]^N \sum_{\{\tau_{x_d}\}} \prod_{\langle x_d y_d \rangle} \left[\tanh \beta \right]^{-\frac{1}{2} \tau_{x_d} \tau_{y_d}}. \quad (71)$$

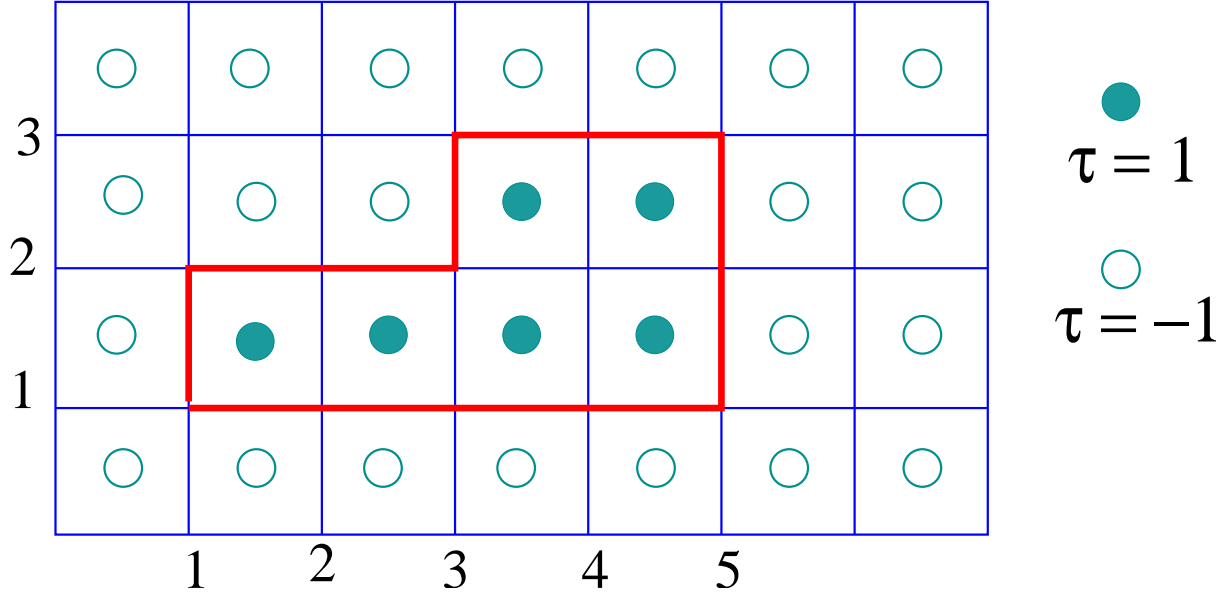


Figure 6: Introducing dual variables to represent closed loops.

This last equation can be written as

$$\mathcal{Z} = \sinh^N(2\beta) \sum_{\{\tau_{x_d}\}} \exp\left\{ \sum_{\langle x_d y_d \rangle} \tilde{\beta} \tau_{x_d} \tau_{y_d} \right\}. \quad (72)$$

$$\tilde{\beta} = -\frac{1}{2} \ln \tanh \beta. \quad (73)$$

We have obtained again a 2d Ising model which is now formulated on the dual lattice: the only difference is that the coupling is now $\tilde{\beta}$ rather than β . It is not generally true that the duality transform yields the same lattice model just with different couplings. Models which *do* have this property are called *self dual*.

Now let us assume that β is large (small temperature). In this case, we find from (73) that

$$\tilde{\beta} \approx e^{-2\beta}, \quad \beta \text{ large.}$$

By contrast, if β is small (the high temperature limit), we find

$$\tilde{\beta} \approx -\frac{1}{2} \ln \beta, \quad \beta \text{ small.}$$

Hence, large β corresponds to small $\tilde{\beta}$ and vice versa (see figure 7). This is interesting since the so-called *strong coupling expansion* techniques are available for small β . Performing the expansion with respect to $\tilde{\beta}$ in the dual model, the large β regime can also be studied by analytic methods. The basis of this expansion is a Taylor expansion of the exponential with respect to β . This expansion naturally reaches its radius of convergence when β

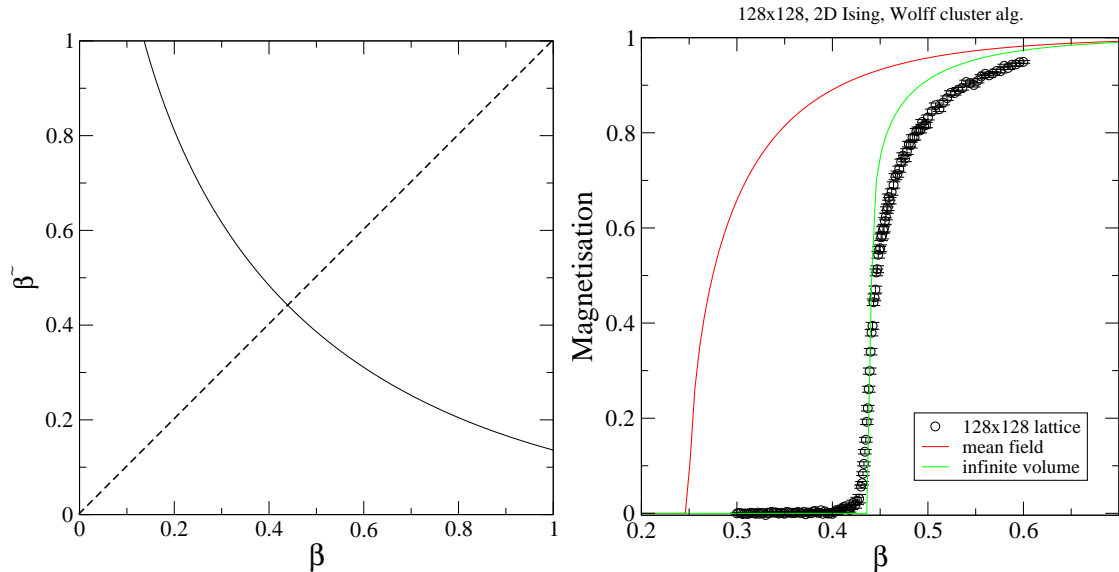


Figure 7: The dual coupling constant $\tilde{\beta}$ as a function of β (left). Magnetisation as a function of β (right).

approaches the critical coupling β_c . Performing the expansion using the dual model, the Taylor expansion with respect to $\tilde{\beta}$ also breaks down at the critical coupling. There are no other couplings for which singularities in thermodynamical quantities occur. Hence, the critical point is obtained if

$$\beta = \tilde{\beta} = \beta_c. \quad (74)$$

Using (73), we therefore find

$$\beta_c = -\frac{1}{2} \ln \tanh \beta_c, \quad \beta_c = \frac{1}{2} \ln(1 + \sqrt{2}) \approx 0.44068679 \dots \quad (75)$$

Figure 7 also shows the magnetisation as a function of β for a 128×128 lattice compared with the mean field result and the exact result in the infinite volume limit.

There are lot of interesting features of field theories already present in the Ising model: there is the relation between a lattice model and a theory of strings, and there is the duality transform which maps the high temperature theory onto a low temperature theory.

3 Markov chain Monte-Carlo: the Ising case study

3.1 Foundations

The idea central to all simulations of lattice models is to generate lattice configurations $\{\sigma_x\}$ according to their probabilistic measure

$$P(\sigma) = \exp(-\beta H(\sigma)) / \mathcal{Z} \quad (76)$$

where \mathcal{Z} is the partition function (55). A straightforward idea to accomplish this task would be to generate randomly the spins at each site x and to accept or reject this configuration according to (76). The problem is that we would hardly find any acceptable configurations. Why is this so?

Let us answer this question in the context of the Ising model of the previous section. The two dimensional lattice consists of $N = 125 \times 125$ sites. Since $\sigma \in \{-1, +1\}$, there are $2^N \approx 10^{4704}$ different lattice configurations. We further introduce the average action per site, i.e.

$$\bar{s} = \frac{1}{N} \left\langle \sum_{\langle xy \rangle} \sigma_x \sigma_y \right\rangle = \frac{1}{N} \left\langle \sum_x \langle \mathcal{A}(x) \rangle \right\rangle = \langle \mathcal{A}(x) \rangle =: \bar{\mathcal{A}} \quad (77)$$

where

$$\mathcal{A}(x) := \sum_{y>x, |x-y|=1} \sigma_x \sigma_y, \quad \sum_{y>x, |x-y|=1} 1 = 2, \quad (78)$$

and where we have used translational invariance. A measure for the strength of the fluctuations of the action around its average value $N \bar{s}$ is given by

$$\delta^2 = \left\langle \left(\sum_{\langle xy \rangle} \sigma_x \sigma_y - N \bar{s} \right)^2 \right\rangle = \left\langle \left[\sum_x (\mathcal{A}(x) - \bar{\mathcal{A}}) \right]^2 \right\rangle \quad (79)$$

$$= \sum_{x,y} \langle (\mathcal{A}(x) - \bar{\mathcal{A}}) (\mathcal{A}(y) - \bar{\mathcal{A}}) \rangle. \quad (80)$$

The crucial observation is that the connected correlation function

$$D(x-y) := \langle (\mathcal{A}(x) - \bar{\mathcal{A}}) (\mathcal{A}(y) - \bar{\mathcal{A}}) \rangle \quad (81)$$

exponentially decreases for large values of $|x-y|$, i.e. $D(x) \propto \exp\{-x/\xi_A\}$, where ξ_A is the correlation length characteristic for fluctuations in the action density. Hence, one finds that its integrated strength, the so-called **susceptibility** ρ , is finite at least for $\beta \neq \beta_c$, i.e.,

$$\rho := \sum_x D(x) < \infty. \quad (82)$$

These findings tell us that the standard deviation δ (80) linearly grows with the number of sites, i.e. $\delta^2 = N \rho$.

Using the central limit theorem to estimate the probability for accepting an action density s , we find

$$P_A \approx \exp\left(-\frac{(Ns - N\bar{s})^2}{\delta^2}\right) = \left[\exp\left(-\frac{(s - \bar{s})^2}{\rho}\right) \right]^N. \quad (83)$$

Hence, in the case of many sites, only configurations with an action per site close to the average action density can significantly contribute to the partition function. If we randomly choose the spins on the sites the action density can take any value between -1 and 1 , and

the argument $(s - \bar{s})/\rho$ is generically of order 1. Hence the acceptance rate is down to $e^{-128 \times 128} \approx 10^{-7115}$.

The basic idea is to only generate configurations which are relevant. Starting from a seed configuration c_0 , we will generate subsequent configurations c_1, c_2, \dots , where the result for c_{i+1} should only depend on the precessing configuration c_i and must not depend on the configurations c_{i-1} . In this case, the set of configurations,

$$c_0 \longrightarrow c_1 \longrightarrow c_2 \longrightarrow c_3 \longrightarrow \dots \longrightarrow c_\infty$$

is called a *Markov chain*. Central ingredient to a Markov chain is the probability $W(b, a)$ with which configuration b is created out of configuration a . This probability must satisfy certain constraints:

- (i) Normalisation $\sum_b W(b, a) = 1, \forall a$
- (ii) Ergodicity $W(b, a) > 0, \forall a, b$
- (iii) Stability $\sum_a W(b, a) P(a) = P(b), \forall b$,

where $P(a)$ is given in (76). If these conditions are met, the series c_i converges to a configuration which is distributed according to $P(c_\infty)$ (76). In order to see this, we introduce the probability $Q_i(c)$ for finding a configuration c at position i of the Markov chain, and denote the deviation from the desired distribution by

$$\epsilon_i = \sum_c \left| Q_i(c) - P(c) \right|. \quad (84)$$

Because of property (ii), there is a W_{\min} with

$$W(a, b) \geq W_{\min} > 0, \quad W'(a, b) := W(a, b) - W_{\min} \geq 0. \quad (85)$$

Furthermore, the condition (i) implies that

$$\sum_c Q_i(c) = 1, \quad \text{as} \quad \sum_c P(c) = 1. \quad (86)$$

Using the stability condition (iii), we then obtain:

$$\begin{aligned} \epsilon_{i+1} &= \sum_c \left| \sum_a W(c, a) Q_i(a) - P(c) \right| = \sum_c \left| \sum_a W(c, a) [Q_i(a) - P(a)] \right| \\ &= \sum_c \left| \sum_a W'(c, a) [Q_i(a) - P(a)] + W_{\min} \sum_a [Q_i(a) - P(a)] \right| \\ &= \sum_c \left| \sum_a W'(c, a) [Q_i(a) - P(a)] \right|. \end{aligned} \quad (87)$$

Using the triangle inequality and the positivity of W' , we find

$$\epsilon_{i+1} \leq \sum_c \sum_a W'(c, a) \left| Q_i(a) - P(a) \right|. \quad (88)$$

Changing the order of summation and using (see (85))

$$\sum_c W'(c, a) = \sum_c (W(c, a) - W_{\min}) = 1 - n_{\text{conf}} W_{\min}, \quad (89)$$

where n_{conf} is the number of configurations, we finally find convergence:

$$\epsilon_{i+1} \leq [1 - n_{\text{conf}} W_{\min}] \sum_a \left| Q_i(a) - P(a) \right| = [1 - n_{\text{conf}} W_{\min}] \epsilon_i. \quad (90)$$

Instead of demanding the less stringent condition (iii), one often demands *detailed balance*:

$$(iii)' \quad W(b, a) P(a) = W(a, b) P(b).$$

The latter condition immediately leads to condition (iii) if we sum the equation (iii)' over the configurations a :

$$\sum_a W(b, a) P(a) = \sum_a W(a, b) P(b) = P(b),$$

where we have used condition (i). Since condition (iii) follows from (iii)' and only (iii) is necessary for our proof above, demanding *detailed balance*, i.e., (iii)', is more restrictive.

3.2 Heat-bath algorithm

The heat-bath algorithm works as follows: (i) randomly choose a site x_0 and consider the corresponding spin $\sigma(x_0)$ for the update. Since the spin only interacts with its nearest neighbours, the interaction can be written as

$$H = \text{const.} - h_0 \sigma_{x_0}, \quad h_0 = \sum_{\langle xx_0 \rangle} \sigma_x. \quad (91)$$

The relative probability for choosing $\sigma(x_0) = 1$ is given by $\exp\{h_0\beta\}$, and the relative probability for $\sigma(x_0) = -1$ is given by $\exp\{-h_0\beta\}$. (ii) Calculate the absolute probability

$$p = \frac{\exp\{\beta h_0\}}{\exp\{-\beta h_0\} + \exp\{\beta h_0\}} \quad (92)$$

with which the spin σ_{x_0} must be set to 1. Choose a random number $z \in [0, 1]$. For $z < p$, choose $\sigma_{x_0} = 1$ otherwise choose $\sigma_{x_0} = -1$. (iii) Subsequently, pick another spin for the update and start again with (i). Once all spins have been visited at least once, one *sweep* has been performed.

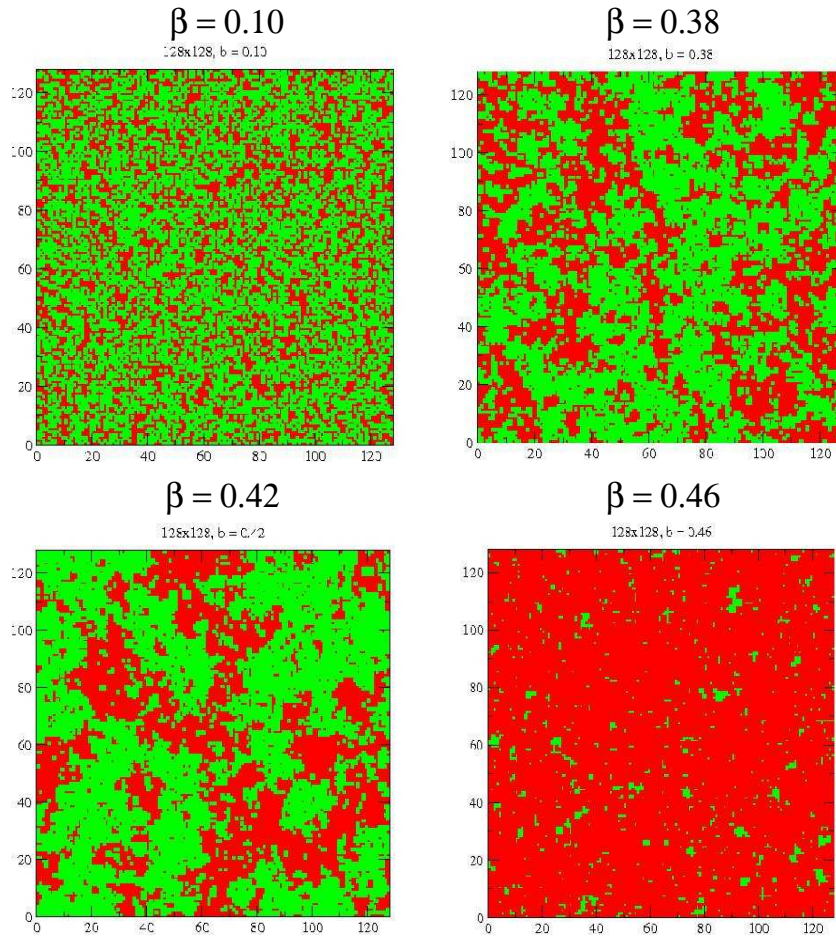


Figure 8: Thermalised spin configurations of the 2d Ising model for several β values starting from high temperature phase to the low temperature ordered phase.

The algorithm above needs an initial configuration. We could choose a unique orientation of all spins. Since this is the ground state of the Hamiltonian which dominates the partition function for small values of the temperature, this initialisation is called a *cold start*. Alternatively, we could start with a random orientation of the spins. This is a configuration which is relevant at very high temperatures where interactions are negligible. This initialisation is therefore called a *hot start*. Independently of our choice, a number of sweeps is carried out to generate a statistically relevant configuration. This procedure is known as *thermalisation*. The number required to arrive at an equilibrated spin lattice depends on the number of degrees of freedom and the temperature.

Let us now examine typical lattice spin configurations. Starting at low β , the sample configurations are highly disordered (see figure 8). Increasing β up to ≈ 0.3 , the clusters of spins with the same orientation already extend over several lattice spacings. Approaching the critical value, e.g. for $\beta \approx 0.42$, the clusters are already as large as the lattice. This

observation reflects the growth of the spin correlation length which, for the present case, is

$$\xi \approx \xi_+ \left| 1 - \frac{T}{T_c} \right|^{-1}, \quad (T \gtrsim T_c), \quad (93)$$

and hence diverges when $\beta \rightarrow \beta_c$.

If our numerical approach should produce the configurations of a Markov chain, the configurations may not depend on the Monte-Carlo history. To find out whether the configurations are indeed statistically independent, we may inspect the autocorrelation time τ e.g. say for the magnetisation M (recall subsection 1.3 for discussions of autocorrelations). To guarantee independence, we perform about 2τ Monte-Carlo sweeps before we consider a configuration eligible for contributing to an estimator. In the case of the heat bath algorithm (in fact, for all local update algorithms), one discovers that the autocorrelation time strongly increases when the critical point is approached. This implies that the interesting regime of the model, namely the regime close to the phase transition, is not accessible with these types of algorithm. The reason for this is the following: consider a spin inside one of the clusters. All the neighbouring spins are pointing in the same direction. If this spin is now subjected to a local update procedure, the spin hardly changes because of the strong mean field produced by the other spins. Hence, only the boundaries of the cluster are significantly modified after one sweep through the lattice. The correct physics is, however, described by configurations consisting of strongly fluctuating clusters. In order to change a cluster completely, there are roughly ξ^2 lattice sweeps necessary. Hence, only after ξ^2 sweeps, the configuration has changed significantly. This, however, implies that the autocorrelation time is roughly given by $\tau \approx \xi^2$. Indeed, it was empirically observed for the Metropolis algorithm that

$$\tau \approx \xi^z, \quad z_{\text{Metro}} \approx 2.125. \quad (94)$$

The index z is called the *dynamical critical exponent* and depends on the algorithm. Since the physical correlation length ξ diverges at the phase transition, (94) implies that the regime near the phase transition cannot be simulated with local update algorithms.

3.3 Cluster update algorithms

State-of-the-art simulations which explore the transition regime use the so-called cluster algorithms. The difference to local update algorithms is that many spins are flipped at a time. To derive the prescription of such a cluster update, we rewrite the partition function (55) as

$$\mathcal{Z} = \sum_{\{\sigma_x\}} \exp \left(\beta \sum_{\langle xy \rangle} \sigma_x \sigma_y \right) = \sum_{\{\sigma_x\}} \prod_{\langle xy \rangle} \exp(\beta \sigma_x \sigma_y). \quad (95)$$

If both neighbouring spins, σ_x and σ_y , in (95) are equal, the probabilistic factor in (95) equals $\exp \beta$. For an opposite orientation of the spins, the probabilistic factor is given by

$\exp(-\beta)$. We therefore cast (95) into

$$\mathcal{Z} = \sum_{\{\sigma_x\}} \prod_{\langle xy \rangle} e^{\beta \left[(1-p) + p \delta_{\sigma_x \sigma_y} \right]}, \quad p := 1 - e^{-2\beta}. \quad (96)$$

We now are going to make the representation of the partition function even more involved by using the identity

$$a + b = \sum_{n=0}^1 \left[a \delta_{n0} + b \delta_{n1} \right].$$

Introducing variables $n_{xy} \in \{0, 1\}$, which are associated with each link of the lattice, we obtain

$$\mathcal{Z} = \sum_{\{\sigma_x\}} \sum_{\{n_{xy}\}} \prod_{\langle xy \rangle} e^{\beta \left[(1-p) \delta_{n_{xy},0} + p \delta_{\sigma_x \sigma_y} \delta_{n_{xy},1} \right]}. \quad (97)$$

The cluster update prescription is now obtained by performing standard heat bath steps for the variables $\{\sigma_x\}$ and $\{n_{xy}\}$.

Let us consider the update for the link variables n_{xy} first. In order to avoid generating a configuration of vanishing probability, we must choose $n_{xy} = 0$ if the neighbouring spins $\{\sigma_x\}$ and $\{\sigma_y\}$ are different (see (97)). If these spins are equally oriented, the probabilistic measure in (97) is given by

$$(1-p) \delta_{n_{xy},0} + p \delta_{n_{xy},1},$$

implying that the link n_{xy} is set to 1 with probability p . Given an initial spin distribution, the values of all link variables can be chosen according to the above prescription.

Let us now consider the spin update. According to probabilistic measure, i.e.,

$$(1-p) \delta_{n_{xy},0} + p \delta_{\sigma_x \sigma_y} \delta_{n_{xy},1},$$

all spins which are connected by links $n_{xy} = 1$ must be of equal orientation. All spins which are connected by so-called activated links, i.e., $n_{xy} = 1$, are said to be part of a cluster. The task is now to find all such clusters on the lattice. Once these clusters have been identified, we assign ± 1 (with equal probability) to all spins of the same cluster.

This first versions of such cluster update algorithms are due to Fortuin and Kasteleyn [5], Swendsen and Wang [6] and Wolff [7]. It is found empirically that the dynamical critical exponent is strongly reduced:

$$\tau \approx \xi^z, \quad z_{\text{cluster}} \approx 0.2. \quad (98)$$

Introductory discussions can be found in [5–8].

4 Quantum field theories on computers

4.1 Quantum mechanics

Let us assume that the motion of a particle of mass m in 1 dimension is governed by a potential $V(x)$. The classical equation of motion can be calculated by variational methods from the action

$$S = \int_0^t dt \left\{ \frac{m}{2} \dot{x}^2 - V(x) \right\}. \quad (99)$$

Classically, these equations of motion determine the time evolution of the position of the particle $x(t)$. At quantum mechanical level, the partition function

$$Z(T) = \text{tr} \exp \left\{ -\frac{1}{T} H \right\} \quad (100)$$

is a convenient starting point to discuss the thermodynamics of the physical system. Here, H is the quantum mechanical Hamiltonian, i.e.,

$$H = -\frac{\hbar^2}{2m} \frac{d^2}{dx^2} + V(x). \quad (101)$$

T is the temperature, and is considered as an external parameter. Once one has succeeded in calculating the partition function (100), thermodynamical quantities can be easily obtained by taking derivatives, e.g., the temperature dependence of the internal energy is given by

$$\langle H \rangle = T^2 \frac{d \ln Z(T)}{dT}. \quad (102)$$

Although a direct calculation of the eigenstates $\langle n|$ of the Hamiltonian might be the easiest way to calculate a quantum mechanical partition function in practical applications, I would like to reformulate (100) in terms of a functional integral. This will be of great help when we generalise the quantum mechanical considerations to the case of a quantum field theory.

For these purposes, I introduce a length scale $L := 1/T$ and an interval $[0, L]$ which I decompose into N equidistant portions of length $a \ll L$, where a is called *lattice spacing*. It is trivial to obtain

$$\exp \left\{ -\frac{1}{T} H \right\} = \exp \left\{ -\sum_{\nu=1}^N a H \right\} = \prod_{\nu=1}^N \exp \{ -a H \}. \quad (103)$$

Let us define complete sets of momentum and position eigenstates ($|p\rangle$ and $|x\rangle$), respectively by

$$1 = \int dx_\nu |x_\nu\rangle \langle x_\nu|, \quad 1 = \int dp_\nu |p_\nu\rangle \langle p_\nu|, \quad (104)$$

for $\nu = 1 \dots N$. As usual, these states obey

$$\langle p_k | x_k \rangle = \exp \left\{ -\frac{i}{\hbar} p_k x_k \right\}.$$

Using a complete set $|x_0\rangle$ of position eigenstates to evaluate the trace in (100), we find

$$\int dx_0 \quad \langle x_0 | \prod_{\nu=1}^N \exp\{-aH\} | x_0 \rangle = \int dx_0 dp_0 dx_1 dp_1 \dots dx_{N-1} dp_{N-1} \\ \langle x_0 | e^{-aH} | p_0 \rangle \langle p_0 | x_1 \rangle \langle x_1 | e^{-aH} | p_1 \rangle \langle p_1 | x_2 \rangle \dots \langle x_{N-1} | e^{-aH} | p_{N-1} \rangle \langle p_{N-1} | x_0 \rangle .$$

Note that the operators p^2 and $V(x)$ do not commute. We may, however, write:

$$\exp \left\{ -a \frac{p^2}{2m} - aV(x) + \frac{a^2}{4m} [V(x), p^2] + \dots \right\} = \exp \{-aV(x)\} \exp \left\{ -a \frac{p^2}{2m} \right\} .$$

Since $|x\rangle$ and $|p\rangle$ are eigenstates of the position operator and momentum operators, respectively, we find

$$\langle x_k | \exp\{-aH\} | p_k \rangle = \exp \left\{ -a \left[\frac{p_k^2}{2m} + V(x_k) + \mathcal{O}(a) \right] \right\} \exp \left\{ \frac{i}{\hbar} p_k x_k \right\} .$$

The partition function therefore becomes up to terms of order a^2

$$Z(T) = \int dx_0 dp_0 dx_1 dp_1 \dots dx_{N-1} dp_{N-1} dx_N \exp \left\{ -a \sum_{k=0}^{N-1} \left[\frac{p_k^2}{2m} + V(x_k) \right] \right\} \\ \exp \left\{ -\frac{i}{\hbar} \sum_{k=0}^{N-1} p_k (x_{k+1} - x_k) \right\} \langle x_0 | x_N \rangle \quad (105)$$

It is straightforward to perform the momentum integrations, which are Gaussian,

$$Z(T) = \left(\frac{4\pi m}{a} \right)^{N/2} \int dx_0 dx_1 \dots dx_N \delta_{x_0 x_N} \\ \exp \left\{ -a \sum_{k=0}^{N-1} \left[\frac{m}{2} \frac{(x_{k+1} - x_k)^2}{a^2 \hbar^2} + V(x_k) \right] \right\} \quad (106)$$

This equation is a completely regularised expression for the partition function and can be directly used in numerical simulations. Note that in the framework of quantum field theory, one sets $\hbar = 1$.

A compact notation can be derived by formally taking the lattice spacing a to zero. For this purpose, we define $a_h := \hbar a$, and the Euclidean action by

$$S_E = \int_0^L d\tau \left\{ \frac{m}{2} \dot{x}^2 + V(x) \right\} . \quad (107)$$

Note the sign change in front of the potential compared with the standard action (99). The interval $[0, L]$, which was introduced above (103), is called *Euclidean time* interval.

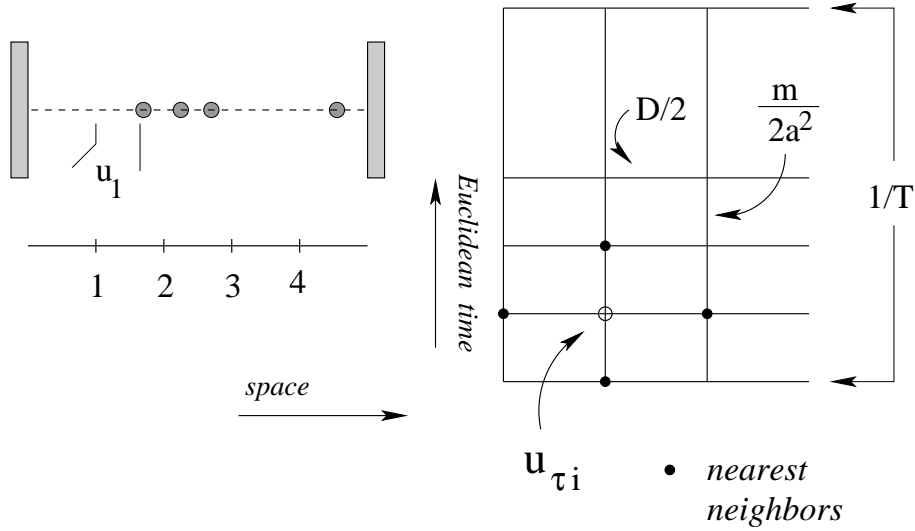


Figure 9: Classical versus quantum partition functions of a 1-dimensional particle chain.

By construction (see above), the length of the Euclidean time interval is given by the inverse temperature, i.e., $L = 1/T$. We also introduce a Euclidean particle trajectory, and a Euclidean velocity

$$x_k \rightarrow x(\tau) \quad \frac{x_{k+1} - x_k}{a_h} \rightarrow \dot{x}(\tau), \quad (108)$$

where we identify $d\tau = a_h$. Using the shorthand notation

$$\left(\frac{4\pi\hbar m}{a_h}\right)^{N/2} \int dx_0 dx_1 \dots dx_{N-1} \rightarrow \mathcal{D}x(\tau),$$

the partition function (106) can be formally written as a functional integral

$$Z(T) = \int \mathcal{D}x(\tau) \exp\left\{-\frac{1}{\hbar} S_E\right\}. \quad (109)$$

Eq.(109) suggests that an average over all Euclidean trajectories $x(\tau)$ must be performed where the probabilistic weight of each trajectory is given by $\exp\{-S_E/\hbar\}$. Note also that in view of the δ -function in (106) only trajectories which are periodic in Euclidean time must be considered, i.e., $x(0) = x(L = 1/T)$.

4.2 Quantum field theory

For illustration purposes, we consider the 1-dimensional particle chain in figure 9. Here, the positions of the particles $i = 0 \dots n$ are characterised by their extensions u_i from the equilibrium position. The particles experience a harmonic potential depending on the

distance to the nearest neighbour. Here, I choose the boundary conditions $u_0 = 0, u_n = 0$. The Hamiltonian, which describes the classical physics, is given by

$$\mathcal{H} = \sum_{i=1}^{n-1} \left[\frac{1}{2m} p_i^2 + \frac{D}{2} (u_{i+1} - u_i)^2 \right]. \quad (110)$$

Hence the classical partition function is given by the multi-dimensional integral

$$Z_{cla}(T) \propto \int dp_1 \dots dp_{n-1} du_1 \dots du_{n-1} \exp \left\{ -\frac{\mathcal{H}}{T} \right\}. \quad (111)$$

In order to calculate the full quantum mechanical partition function of the particle chain, we first write down the Euclidean partition function. Note for this purpose that the displacements u_i now acquire an additional dependence on the Euclidean time $u_i \rightarrow u_i(\tau) \equiv u_{\tau i}$. With this notation the Euclidean action is given by

$$S_E = \sum_{\tau=1}^N \sum_{i=1}^{n-1} a \left[\frac{m}{2a^2} (u_{\tau,i} - u_{\tau-1,i})^2 + \frac{D}{2} (u_{\tau,i+1} - u_{\tau,i})^2 \right]. \quad (112)$$

The interactions between the c-number fields $u_{\tau i}$ can be easily visualised (see figure 9): the fields $u_{\tau i}$ harmonically interact with their nearest neighbours. The harmonic interaction strength is given by $D/2$ in space direction and $m/2a^2$ for neighbours in Euclidean time direction. The quantum mechanical partition function can be calculated by integrating over the fields $u_{\tau i}$ located at the sites of a 2-dimensional grid, .i.e.

$$Z(T) \propto \int \mathcal{D}u \exp \{ -S_E \}, \quad (113)$$

where the temperature enters the consideration via the extension of the lattice in Euclidean time direction with fields obeying periodic boundary conditions.

To conclude, we observe that the partition function of a classical $D + 1$ dimensional field theory (in lattice regularisation) describes the full partition function of a D dimensional quantum system. D is the number of space dimensions. This correspondence is very helpful in understanding the quantum behaviour of a theory, since it can be mapped to a classical field theory (at the expense of an additional dimension). In the next section, we will study classical partition functions in 4-dimensional Euclidean space in order to derive the information on the thermodynamics of the full quantum system.

5 Lattice gauge theory

5.1 The gauged Ising model

The Ising model, strictly speaking the partition function (55), is invariant under the *global* transformation of the spins given by

$$\sigma^\Omega(x) = \Omega \sigma(x), \quad \Omega = \pm 1. \quad (114)$$

The transformation is called *global* because the transformation affects all spins at the same time, i.e., Ω is independent of the coordinates (sites). The corresponding symmetry group is Z_2 .

This symmetry group can be generalised to a *local* symmetry, also known as *gauge symmetry*, by demanding invariance under

$$\sigma^\Omega(x) = \Omega(x) \sigma(x), \quad \Omega(x) = \pm 1. \quad (115)$$

Of course, the action (56) of the standard Ising model is not invariant under the huge symmetry group which is now $[Z_2]^N$, where N is the number of sites. In order to obtain a version of the Ising model which possesses a Z_2 gauge symmetry, we need to change the action. The only way to do it, is to introduce an additional field, $Z_\mu(x)$. This field is associated with the links of the lattice: x specifies the site and μ the direction in which we find the link. Alternatively, we could write:

$$Z_\mu(x) = Z_{\langle xy \rangle}, \quad y = x + \hat{e}_\mu,$$

where \hat{e}_μ is the unit vector in μ direction. For the latter expression, we will also abbreviate

$$x + \hat{e}_\mu = x + \mu.$$

For the action, we choose

$$S_{\text{matter}} = \kappa \sum_{\langle xy \rangle} \sigma(x) Z_\mu(x) \sigma(x + \mu), \quad (116)$$

and demand that the link Z_μ transforms under gauge transformations as

$$Z_\mu^\Omega(x) = \Omega(x) Z_\mu(x) \Omega(x + \mu). \quad (117)$$

Since spin and link transform simultaneously with the same $\Omega(x)$ and since $\Omega^2(x) = 1$, one easily proves the gauge invariance of the action (116).

Obviously, the action S_{matter} describes the interaction between the *matter* fields, i.e., the spins, and the new link fields. What is left to do is to design a gauge invariant action for these new degrees of freedom. This interaction should be short ranged in order to preserve some desirable features such as universality. A possible choice is

$$S_{\text{link}} = \beta \sum_{x, \mu > \nu} P_{\mu\nu}(x), \quad P_{\mu\nu}(x) = Z_\mu(x) Z_\nu(x + \mu) Z_\mu(x + \nu) Z_\nu(x). \quad (118)$$

Here, the numbers $(x, \mu > \nu)$ specify the plaquette of the lattice the lower left corner of which is located at site x and which is spanned by the directions μ and ν . The field combination $P_{\mu\nu}(x)$ is often called the plaquette for short. The proof that $P_{\mu\nu}(x)$ is indeed invariant under gauge transformations (117) is left to the reader.

The total action of the gauged Ising model consists of two parts: the matter part and the “gauge” part. Correspondingly, there are two coupling constants: the convention is that β is the pre-factor in the pure gauge action, while κ multiplies the matter part.

Once our system is now gauged, it only makes sense to consider gauge invariant observables since non-gauge invariant quantities vanish. Let us explore this for a simple gauge variant quantity such as the spin correlation function:

$$C(x_0, y_0) = \frac{1}{\mathcal{Z}} \sum_{\{\sigma\}} \sigma(x_0) \sigma(y_0) \exp \{S[\sigma]\}, \quad S[\sigma] = S_{\text{matter}} + S_{\text{link}}, \quad (119)$$

$$\mathcal{Z} = \sum_{\{\sigma\}} \exp \{S[\sigma]\}, \quad (120)$$

Let us now consider a particular gauge transformation (115) of the spins, i.e.,

$$\Omega(x) = \begin{cases} -1 & \text{for } x = x_0 \\ 1 & \text{else} \end{cases} \quad (121)$$

Renaming all spins in the sum in (119) by $\sigma(x) \rightarrow \sigma^\Omega(x)$, we use the gauge invariance of the action and the sum, i.e.,

$$S[\sigma] = S[\sigma^\Omega], \quad \sum_{\{\sigma\}} = \sum_{\{\sigma^\Omega\}}.$$

The sum is trivially invariant, since we sum anyhow over all possible ± 1 combinations for the spins. Thus, we obtain:

$$\begin{aligned} C(x_0, y_0) &= \frac{1}{\mathcal{Z}} \sum_{\{\sigma\}} \sigma^\Omega(x_0) \sigma^\Omega(y_0) \exp \{S[\sigma]\} \\ &= \frac{1}{\mathcal{Z}} \sum_{\{\sigma\}} [-\sigma(x_0)] \sigma(y_0) \exp \{S[\sigma]\} = -C(x_0, y_0), \end{aligned} \quad (122)$$

where we used our particular choice (121) in the last line above. We conclude from this that $C(x_0, y_0) = 0$.

5.2 Pure Z_2 gauge theory: 3 and 4 dimensions

Let us now consider the particular case $\kappa = 0$ when the matter fields are absent from the theory. The emerging theory is called *pure* Z_2 gauge theory, and it is a theory of link fields only. What are the physical (i.e. gauge invariant) degrees of freedom in this case? Let us consider the more interesting case of 3 and 4 dimensions for these considerations. In order to talk about gauge invariant information, we now consider the plaquettes P_p , $p = (x; \mu\nu)$, defined in (118). We say that a short flux line (vortex) passes through the plaquette p if

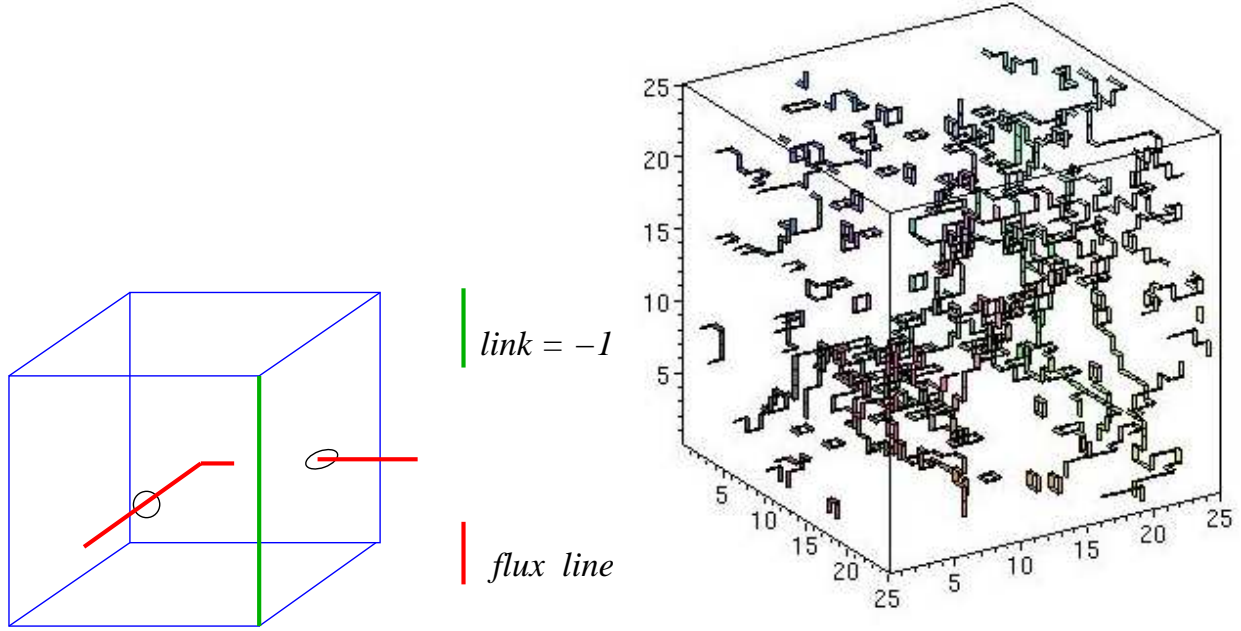


Figure 10: Flux passing through an elementary cube (left) and closed flux lines on a 3d lattice (right).

$P_p = -1$. Since the plaquette variables P are gauge invariant, so are the flux lines. More formally, we introduce a vortex plaquette variable by

$$v_p = \prod_{l \in p} Z_l \quad (123)$$

and consider the flux lines which enter/leave an elementary cube of the lattice. We take the product of all vortex plaquettes which are associated with the faces of the elementary cube and find

$$\prod_{p \in c} v_p = (-1)^\nu, \quad (124)$$

where ν is the total number of vortices at the faces of the cube. Inserting the definition (123), we also find that

$$\prod_{p \in c} v_p = \prod_{p \in c} \prod_{l \in p} Z_l = 1, \quad (125)$$

since in the latter products all Z_l factors appear twice (see figure 10, left panel; remember $Z_l^2 = 1$). Comparing (125) with (124), we realise that ν must be even. In particular, $\nu = 1$ is excluded implying that a vortex never ends inside a cube. Considering 3 dimensions (or the spatial hypercube of 4-dimensional space time), we find that the gauge invariant vortices form closed lines in space. See figure 10, right panel, for an illustration.

4 dimensions: Let us consider the 4 dimensional model first. The constraint (125) is most easily interpreted on the dual lattice. A plaquette p of the original lattice maps onto

a plaquette $*p$ of the dual lattice, and a cube c corresponds to a link $*l$ on the dual lattice. Hence, the constraint (125) reads on the dual lattice

$$\prod_{*p \in *l} v_{*p} = 1. \quad (126)$$

This simply means that the number of vortex plaquettes which are attached to a link on the dual lattice must be even. Accordingly, the vortex plaquettes form closed surfaces on the dual lattice. If n denotes the number of negative plaquettes on the original lattice, the number of trivial plaquettes in 4 dimension is $6N - n$, where N is the number of lattice points. Hence, the probabilistic weight of such a configuration is:

$$[\exp\{\beta\}]^{6N-n} [\exp\{-\beta\}]^n = \exp\{6N\beta\} \exp\{-2\beta n\},$$

so that the partition function can be written as

$$\mathcal{Z} = \exp\{6N\beta\} \sum_{\{\text{closed surfaces}\}} \exp\{-2\beta n\}. \quad (127)$$

Let us interpret this partition function: the degrees of freedom are closed two dimensional sheets (2-branes) embedded in four dimensions. The surface A of these branes is given by n . Hence, the probabilistic factor is given by

$$\exp\{-2\beta A\}$$

implying that 2β can be interpreted as the *surface tension*. At zero temperature ($\beta \rightarrow \infty$), the empty vacuum (no 2-branes) is realised. At finite temperatures, the brane entropy competes with the penalty from the weight factor. A direct calculation of the entropy of 2d world-sheets in 4d would be cumbersome. However, exploiting the relation to the Z_2 gauge theory makes the calculation of brane expectation values easily accessible by numerical means.

Let us proceed to obtain the duality map of the 4d Z_2 gauge theory. The basic trick to perform the sum over the closed surfaces is to introduce degrees of freedom which automatically resolve the constraint. In the present case, these are links $*Z_{*l}$ on the dual lattice. Let us consider

$$\sum_{\{*Z_{*l}\}} \prod_{*p} [1 + t P_{*p}[*Z]], \quad (128)$$

where $P_{*p}[*Z]$ is the plaquette generated by the links $*Z$ on the dual lattice. When we remove the brackets in (128), the only way to have a non-vanishing contribution to the sum is by making sure that each link $*Z_{*l}$ appears an even number of times. This, however, means that the negative plaquettes $P_{*p}[*Z]$ form closed surfaces. Hence, we find

$$\sum_{\{*Z_{*l}\}} \prod_{*p} [1 + t P_{*p}[*Z]] = 2^{4N} \sum_{\{\text{closed surfaces}\}} t^n. \quad (129)$$

Note that there are $4N$ links on the 4 dimensional lattice and that the factor 2^{4N} arises from the sum over ${}^*Z_{*l}$. Thus, using (129) in (127), we find

$$\mathcal{Z} = \exp\{6N\beta\} 2^{-4N} \sum_{\{{}^*Z_{*l}\}} \prod_{*p} \left[1 + t P_{*p}[{}^*Z]\right], \quad t = \exp\{-2\beta\}. \quad (130)$$

Since the plaquette $P_{*p}[{}^*Z]$ only acquires values ± 1 , we may write:

$$\prod_{*p} \exp\{\tilde{\beta} P_{*p}[{}^*Z]\} = [\cosh \tilde{\beta}]^{6N} \prod_{*p} \left[1 + \tanh \tilde{\beta} P_{*p}[{}^*Z]\right]. \quad (131)$$

The partition function (130) therefore becomes

$$\mathcal{Z} = \left[\frac{\exp\{\beta\}}{\cosh \tilde{\beta}}\right]^{6N} 2^{-4N} \sum_{\{{}^*Z_{*l}\}} \exp\left\{\tilde{\beta} \sum_{*p} P_{*p}[{}^*Z]\right\}, \quad (132)$$

$$\exp\{-2\beta\} = \tanh \tilde{\beta}. \quad (133)$$

First of all we note that the dual of pure Z_2 gauge theory is another 4-dimensional Z_2 gauge theory: the model is self-dual. Furthermore, relation (133) is already familiar to us: we have obtained a complete analogue of the relation between β and its dual $\tilde{\beta}$ for the 2d Ising model. We therefore once again encounter the fact that the weak coupling regime is mapped to the strong coupling regime of the same model. As a byproduct we find that the critical coupling is given by

$$\beta_c = \frac{1}{2} \ln(1 + \sqrt{2}) \approx 0.44068679 \dots \quad (134)$$

The fact that the critical couplings of the 2d Ising model and 4d pure Z_2 gauge theory coincide might be a numerical accident. At least, I do not know any deeper reason for it. I finally point out that the Z_2 gauge symmetries of the original and the dual formulation are completely unrelated. This can be most easily seen from the fact that, at an intermediate stage, we have formulated the model entirely in terms of physical, i.e., gauge invariant variables: the closed vortex sheets of the dual lattice. Resolving this constraint, the gauge invariance of the dual model arose from a parameterisation invariance, namely, the redundancy when we performed the sum over all closed world sheets with the help of dual gauge links *Z .

3 dimensions: Let us finally discuss the 3-dimensional model. In 3 dimensions, a plaquette p is mapped to a link *l and a cube c is mapped to a site *x on the dual lattice. The constraint (125) then translates to

$$\prod_{{}^*l \in {}^*x} v_{*l} = 1. \quad (135)$$

The plaquettes carrying negative flux on the original lattice are represented by links forming closed loops on the dual lattice. The partition function now takes the form (there are $3N$ links on the lattice):

$$\mathcal{Z} = \exp\{3N\beta\} \sum_{\{\text{closed loops}\}} \exp\{-2\beta n\} . \quad (136)$$

We already know how to perform the sum over all closed loops from subsection 2.4:

$$\begin{aligned} & 2^{-3N} \sum_{\{\tau_{*x}\}} \prod_{*l} \exp\{\tilde{\beta} \tau_{*x} \tau_{*y}\} \\ &= \left[\frac{\cosh \tilde{\beta}}{2} \right]^{3N} \sum_{\{\tau_{*x}\}} \prod_{*l} [1 + \tanh \tilde{\beta} \tau_{*x} \tau_{*y}] = [\cosh \tilde{\beta}]^{3N} \sum_{\{\text{closed loops}\}} [\tanh \tilde{\beta}]^n . \end{aligned} \quad (137)$$

Identifying once again

$$\exp\{-2\beta\} = \tanh \tilde{\beta} , \quad (138)$$

we find

$$\mathcal{Z} = \left[\frac{\exp\{\beta\}}{2 \cosh \tilde{\beta}} \right]^{3N} \sum_{\{\tau_{*x}\}} \exp\left\{ \sum_{*l} \tilde{\beta} \tau_{*x} \tau_{*y} \right\} . \quad (139)$$

Obviously, the Z_2 gauge theory is dual to a theory which is not a gauge theory anymore, the 3d Ising model. This has tremendous consequences: for the standard Ising model, cluster update algorithms are available. Using the Swendsen-Wang or Wolff type cluster update, we are able to simulate a gauge theory with much less autocorrelations. Unfortunately, such a framework is not (yet) available for more relevant theories such as lattice Yang-Mills theories.

5.3 Setting up lattice Yang-Mills theory

Due to the universality conjecture, the lattice model with the correct number of dimensions and the correct symmetries uniquely defines the corresponding quantum field theory in the critical limit. The purpose of the present subsection is to propose a classical lattice model which satisfies these prerequisites in the case of Yang-Mills theory.

The QCD matter fields (quarks) belong to the fundamental representation of the so-called $SU(N_c)$ colour group ($N_c = 3$ for QCD). **Gauge invariance** means that the action of the quark fields is invariant under the *local* unitary transformations, i.e.,

$$q(x) \rightarrow q'(x) = \Omega(x) q(x), \quad \Omega(x) \in SU(N_c) . \quad (140)$$

As explained in many text books, local gauge invariance of the quark kinetic term may only be achieved by introducing additional dynamical fields, the gluon fields $A_\mu(x)$.

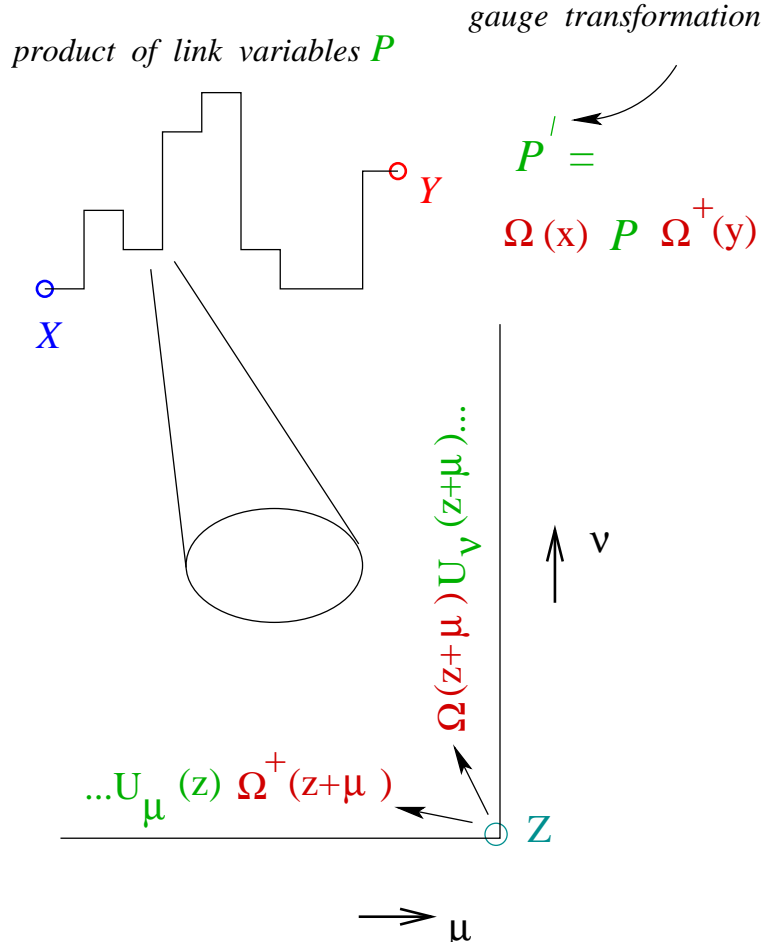


Figure 11: Path ordered product of link variables.

The quark fields are associated with the sites in a lattice formulation. Hence, the symmetry group of the classical lattice Yang-Mills model is $[SU(N_c)]^{N_s}$, where N_s is the number of lattice sites. In order to enforce such a high symmetry in the critical limit of a lattice model, it has turned out essential to realise the symmetry even for finite values of the lattice spacing a . This in turn forces the model to maintain local gauge invariance in the continuum limit [9]. A potential candidate for a quark kinetic term in the non-interacting case is

$$\sum_{x,\mu} \frac{1}{2} \left[\bar{q}(x) \gamma_\mu q(x+\mu) - \bar{q}(x+\mu) \gamma_\mu q(x) \right], \quad (141)$$

where the γ_μ are the Euclidean γ matrices. Of course, the action (141) is not invariant under the gauge transformations (140). To achieve this invariance, we introduce an additional field of vector type, thus being related to the links of the lattice,

$$U_\mu(x) \in SU(N_c). \quad (142)$$

$$\mathbf{P}_{\mu\nu}(\mathbf{x}) = \frac{1}{N_c} \text{tr} \left[\text{square with loop} \right]$$

plaquette

Figure 12: Lattice plaquette variable

Generalising the quark kinetic term (141) to

$$S_Q = \sum_{x,\mu} \frac{1}{2} \left[\bar{q}(x) \gamma_\mu U_\mu(x) q(x + \mu) - \bar{q}(x + \mu) \gamma_\mu U_\mu^\dagger(x) q(x) \right], \quad (143)$$

one obtains the desired local invariance upon demanding that the link fields transform as

$$U_\mu(x) \rightarrow \Omega(x) U_\mu(x) \Omega^\dagger(x + \mu). \quad (144)$$

Let us follow the case of the gauged Ising model and construct a kinetic term for the link fields $U_\mu(x)$. For lattice models “kinetic” means that the interactions of the fields on the lattice are *short range*, i.e., only nearest neighbours are involved. In order to design a gauge invariant kinetic term for every value of the lattice spacing, we firstly investigate the transformation properties of a path ordered product of link variables. Let us consider an open path C which starts at point x and ends at y (see figure 11 for an illustration), and define

$$P(x, y) = \mathcal{P} \prod_{x \in C} U(x), \quad (145)$$

where \mathcal{P} implies path ordering. Inserting the gauge transformed links (144) into (145), one finds

$$P(x, y) \rightarrow P'(x, y) = \Omega(x) P(x, y) \Omega(y). \quad (146)$$

With the help of (145), it is easy to construct a kinetic term for the link variables which (i) is gauge invariant and (ii) involves only next to nearest neighbours. For this purpose one chooses C to be a closed path starting at x and ending at $y = x$ which encircles an elementary **plaquette** (see figure 12):

$$\begin{aligned}
P_{\mu\nu}(x) &= \frac{1}{N_c} \text{tr} P(x, y) \\
&= \frac{1}{N_c} \text{tr} \left\{ U_\mu(x) U_\nu(x + \mu) U_\mu^\dagger(x + \nu) U_\nu^\dagger(x) \right\}. \quad (147)
\end{aligned}$$

Using (146) and the invariance of the trace under cyclic permutations, one easily shows that the plaquette (147) is indeed gauge invariant.

The lattice partition function involves an integration over the dynamical fields of the theory. In the case of the group valued link variables (142), the question arises which measure $\mathcal{D}U_\mu$ should be employed for the integrations. We must demand that the integration measure does not spoil gauge invariance. To ensure this we use the so-called Haar measure which satisfies

$$dU_\mu(x) = d\left(AU_\mu(x)B\right), \quad A, B \in SU(N_c). \quad (148)$$

The Haar measure is available in closed form for the unitary groups $SU(N_c)$. Here, I will only present the Haar measure for $SU(2)$ group integrations. The $SU(2)$ unitary matrix U is conveniently parameterised in terms of the Pauli matrices,

$$U = a_0 + i \vec{a} \vec{\tau}, \quad UU^\dagger = 1 \rightarrow a_0^2 + \vec{a}^2 = 1. \quad (149)$$

Since the constraint $UU^\dagger = 1$, i.e. $a_0^2 + \vec{a}^2 = 1$, is not changed if U is multiplied with A from the left and B from the right, respectively, these multiplications can be viewed as rotations in the 4-dimensional space spanned by (a_0, \vec{a}) . Therefore, an invariant measure can be defined by

$$dU = da_0 da_1 da_2 da_3 \delta\left(a_0^2 + \vec{a}^2 - 1\right). \quad (150)$$

Introducing polar coordinates for the 3-dimensional vector $\vec{a} := a\vec{n}$, $\vec{n}\vec{n} = 1$, the integration over the norm of the vector \vec{a} can be performed with the help of the δ function in (150). We obtain the final result for the $SU(2)$ Haar measure, i.e.,

$$dU = da_0 \sqrt{1 - a_0^2} d\Omega_{\vec{n}}, \quad (151)$$

which is commonly used in lattice simulations.

Finally, the lattice representation of the gauge invariant partition function is given by

$$Z = \int \mathcal{D}U \mathcal{D}q \mathcal{D}q^\dagger \exp\left\{-S_Q + \beta \sum_{x,\mu>\nu} \frac{1}{2} [P_{\mu\nu}(x) + \text{h.c.}]\right\}, \quad (152)$$

where the quark interaction is encoded in S_Q (143) and $P_{\mu\nu}(x)$ is the plaquette (147). β is related to the bare gauge coupling constant g of the continuum formulation by $\beta = 2N_c/g^2$. The particular choice (152) of the lattice regularised gluonic action is known as the *Wilson action* [9]. Note that the fields $q(x)$, $q^\dagger(x)$ are anti-commuting Grassmann fields. This choice for the fermionic fields is necessary to obtain the correct Fermi statistics as well as to ensure the Pauli principle. It implies that the lattice model (152) cannot be straightforwardly be used in numerical simulations. Rather, since the action for the quark fields is quadratic, the integration over the quark fields has to be performed analytically:

$$\int \mathcal{D}q \mathcal{D}q^\dagger \exp\left\{-\bar{q}_A M_{AB} q_B\right\} = \text{Det}M[U]. \quad (153)$$

where the index A comprises space-time as well as spinorial, etc. indices. The quark determinant $\text{Det}M[U]$ is a gauge invariant function of the link variables $U_\mu(x)$. Note, however, that the link interaction mediated by the quark determinant is non-local, implying that a link at a particular site is coupled to all other links of the lattice. In practice, this implies that a local update of a single link enforces the calculation of a functional determinant. This explains why the numerical simulation of Yang-Mills theory with dynamical quarks requires much more computational resources than the simulation of the theory in **quenched approximation**, where the quark determinant is neglected for the update of the link variables.

5.4 The fermion doubling problem

It turns out that the treatment of the quark degrees of freedom in (152) is still too naive: since the Dirac equation is linear in momentum, its lattice analogue does not produce just the desired quark degrees of freedom in the limit $a \rightarrow 0$, but rather 2^D copies of them (D is the number of space time dimensions). This is already true for the free theory as will be shown in what follows.

Let us firstly introduce the generating functional for connected Green functions in the case of free and massless bosonic theory,

$$Z[j] = \int \mathcal{D}\phi \exp \left\{ -\frac{1}{2} \phi_k \Pi_{kl} \phi_l + j_x \phi_x \right\}. \quad (154)$$

A sum is understood over indices which appear twice. One easily verifies that the connected correlation function is obtained from $Z[j]$ via

$$f(x-z) := \langle \phi_x \phi_z \rangle - \langle \phi_x \rangle \langle \phi_z \rangle = \frac{d \ln Z[j]}{dj_x dj_z}. \quad (155)$$

By “completing the square” in (154), we find

$$Z[j] \propto \exp \left\{ \frac{1}{2} j_x \left(\Pi^{-1} \right)_{xz} j_z \right\}, \quad (156)$$

and hence for the free bosonic case

$$\langle \phi_x \phi_z \rangle - \langle \phi_x \rangle \langle \phi_z \rangle = \left(\Pi^{-1} \right)_{xz}. \quad (157)$$

In order to evaluate the inverse Π^{-1} , of the ”kinetic” operator, we introduce its eigenvalues and eigenvectors, whereupon

$$\Pi |k\rangle = \lambda_k |k\rangle, \quad (158)$$

and formally write

$$\left(\Pi^{-1} \right)_{xz} = \sum_k |k\rangle \frac{1}{\lambda_k} \langle k|. \quad (159)$$

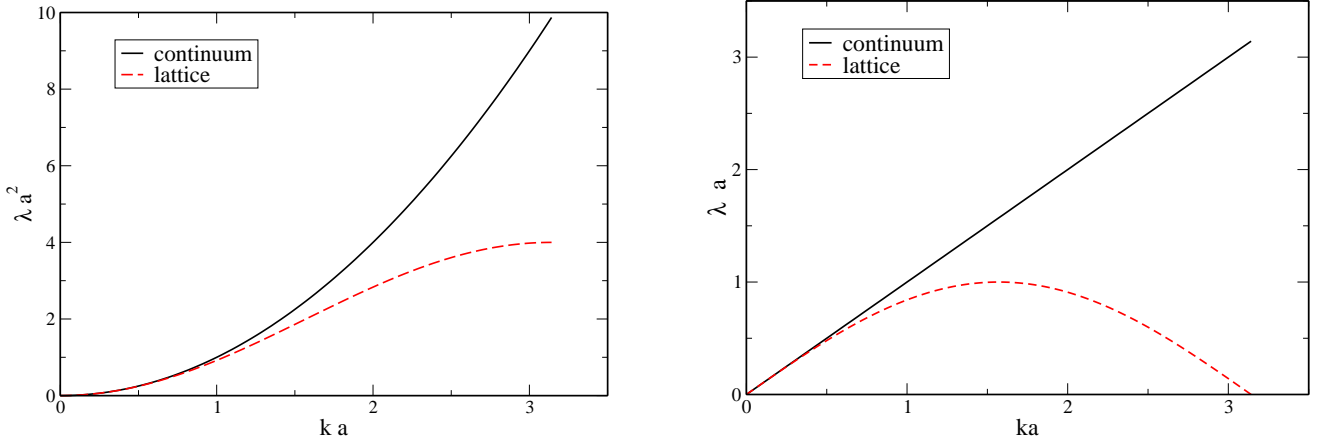


Figure 13: Dispersion relation from the tree level kinetic term (continuum versus lattice formulation) for the bosonic case (left) and the fermionic case (right panel).

It is now easy to calculate the correlation function for the continuum case $\Pi = -\partial^2$. The eigenfunctions are subjected to periodic boundary conditions $\phi(x) = \phi(x + L)$, i.e.,

$$\phi(x) \propto e^{ikx}, \quad e^{ikL} = 1, \quad k = \frac{2\pi}{L}n, \quad n \in Z. \quad (160)$$

The discrete k levels are called **Matsubara frequencies**. In the continuum, there are no further restrictions on the integer n . Making the ansatz (160), we find that the eigenvalues are given by

$$\lambda(k) = k^2 \quad (\text{continuum}). \quad (161)$$

Hence, a free massless particle manifests itself in the correlation function (159) as a pole at zero momentum transfer. The lattice version of the eigenvalue equation is

$$\Pi\phi(x) = \sum_{\mu} \left[-\phi(x + \mu) + 2\phi(x) - \phi(x - \mu) \right] = \lambda_{latt} a^2 \phi(x). \quad (162)$$

In order to solve this equation, we use the plane wave ansatz (160). One crucial difference between the lattice and the continuum version is that only wavelengths l obeying

$$\frac{l}{2} \geq a, \quad \frac{\pi}{k} \geq a \quad (163)$$

are sensible. The lattice naturally provides an UV momentum cutoff, i.e., $\Lambda_{UV} = \pi/a$. Inserting (160) into (162) one finds

$$\lambda_{latt} a^2 = \sum_{\mu} \left[2 - e^{ik_{\mu}a} - e^{-ik_{\mu}a} \right] = 4 \sum_{\mu} \sin^2\left(\frac{k_{\mu}a}{2}\right). \quad (164)$$

For momenta which are small compared to the UV cutoff, i.e., $ka \ll \pi$, we recover the continuum dispersion relation

$$\lambda_{latt} = k^2 \left[1 + \mathcal{O}(k^2 a^2) \right]. \quad (165)$$

In figure 13 the continuum dispersion relation for bosons is compared to its lattice version. The lattice correlation function has only one singularity reflecting that in the scaling limit $\lambda a^2 \ll 1$, $ka \ll \pi$, the dispersion relation of the continuum free particle is recovered.

Let us move on to the fermionic case. In order to reproduce the correct Fermi statistics, fermion fields $\psi(x)$ are of Grassmann type and obey anti-periodic boundary conditions. I refer to the textbook [2] for an introduction to the free fermionic theory, and only quote the final result for the correlation function which formally agrees with (159). In the continuum, the eigenvalue equation is given by

$$\Pi\psi(x) = \not{\partial}\psi(x) = \lambda\psi(x), \quad (166)$$

where anti-hermitian (Euclidean) γ matrices are used. The ansatz for the spinor wave functions is again of plane wave type,

$$\psi(x) \propto u(k) e^{ikx}, \quad e^{ikL} = -1, \quad k = \frac{2\pi}{L} \left(n + \frac{1}{2} \right), \quad n \in Z. \quad (167)$$

The spectrum $\lambda(k)$ is determined by making the ansatz

$$u(k) = \left[i\not{k} + \lambda \right] u_0, \quad (168)$$

which yields

$$\left[i\not{k} - \lambda \right] u(k) = \left[i\not{k} - \lambda \right] \left[i\not{k} + \lambda \right] u_0 = 0, \quad (169)$$

and therefore

$$\left[k^2 - \lambda^2 \right] u_0 = 0. \quad (170)$$

Hence, the spectrum of the continuum theory is linearly increasing, $\lambda = \pm\sqrt{k^2}$. Using the kinetic energy for a free quark theory introduced in (141), the lattice version of the eigenvalue equation is given by

$$\frac{1}{2} \sum_{\mu} \left[\gamma_{\mu} \psi(x + \mu) - \gamma_{\mu} \psi(x - \mu) \right] = \lambda a \psi(x). \quad (171)$$

The ansatz (167) also provides the eigenvectors of the eigenvalue problem (171). Repeating the steps which have led to the continuum dispersion relation, one finds its lattice analogue

$$\lambda a = \sqrt{\sum_{\mu} \sin^2(k_{\mu} a)}. \quad (172)$$

The fermionic eigenvalue distribution is shown in figure (13), right panel. Close to the critical limit ($\lambda a \ll 1$), one recovers the continuum dispersion relation from (172) by making a Taylor expansion with respect to ka . In addition, a second singularity occurs for $ka \approx \pi$. This shows that even if $\lambda a \ll 1$ a second fermion flavour arises from the lattice fermion action (141).

It can be shown that this fermion doubling problem must occur for a chirally invariant action which is translationally invariant and local (**Nielsen-Ninomiya No-Go theorem**). At the present stage, a lot of research effort is devoted to incorporate chiral symmetry at the expense of, say, a moderate non-locality of the action [10].

5.5 Overlap fermions

In the continuum formulation, the chirally invariant Dirac operator \mathcal{D} satisfies the relations

$$\{\mathcal{D}, \gamma_5\} = 0, \quad \{\mathcal{D}^{-1}, \gamma_5\} = 0, \quad (173)$$

which tells us that the non-zero eigenvalues $\bar{\lambda}$ appear in pairs $\{\bar{\lambda}, -\bar{\lambda}\}$. Let D denote a lattice candidate of the Dirac operator (in units of the lattice spacing a) satisfying the so-called *Ginsparg-Wilson relation* [11],

$$\{D, \gamma_5\} = 2 D \gamma_5 D. \quad (174)$$

One observes that the right hand side of (174) is of order a^2 (compared with the order a of the left hand side) implying that the naive continuum limit $a \rightarrow 0$ of (174) reduces to the chiral relation (173). The most important observation, however, is that a certain remnant of the chiral symmetry is still present in the lattice version. Defining

$$\tilde{D}^{-1} := D^{-1} - 1, \quad (175)$$

and using

$$\{\gamma_5, D^{-1}\} = 2 \gamma_5,$$

which directly follows from the Ginsparg-Wilson relation (174), we observe that \tilde{D}^{-1} may be used as a chirally invariant quark propagator, i.e.,

$$\{\gamma_5, \tilde{D}^{-1}\} = 0. \quad (176)$$

Hence, we are left with the task to find an operator D obeying the Ginsparg-Wilson relation (174). Here, I will briefly discuss the Overlap Dirac operator [12]- [14], firstly introduced in the pioneering paper [12] by Narayanan and Neuberger. One introduces

$$D = \frac{1}{2} [1 + \gamma_5 H], \quad (177)$$

where H is a Hermitian operator with eigenvalues ± 1 . Common choice is

$$H = D_w / \left(D_w^\dagger D_w \right)^{1/2}, \quad (178)$$

where D_w is the standard Hermitian Wilson-Dirac operator. Inserting (177) into (174), it is straightforward to prove that D from (177) satisfies the Ginsparg-Wilson relation (174). A comprehensive discussion of the quark propagator (175) in the context of a simulation of SU(3) Yang-Mills theory can be found in [15].

Wilson loop:

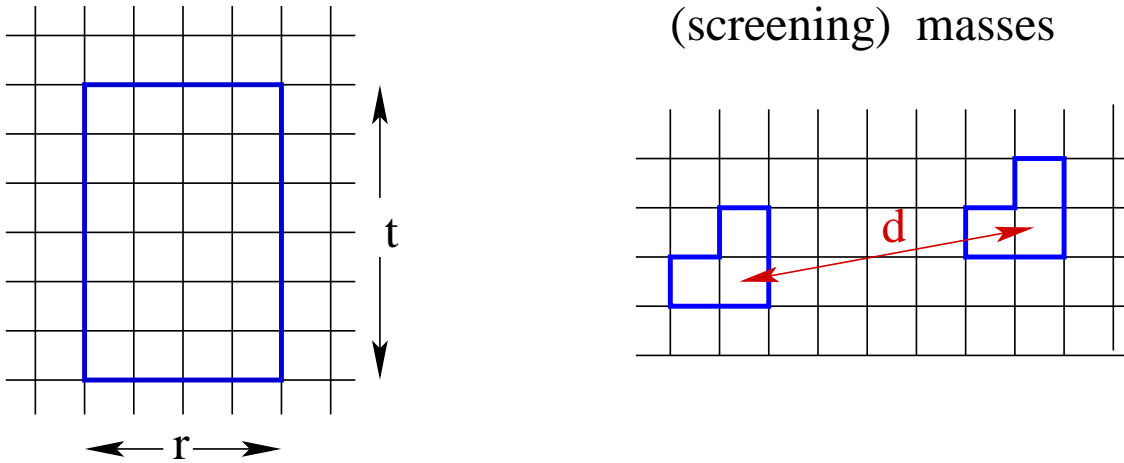


Figure 14: Wilson loop and loop–loop correlation function

5.6 Measuring observables

We have observed that the trace of the path ordered product $P(x, y)$ of link variables (145) is gauge invariant when taken along a closed curve C , i.e., $x = y$. Depending on the choice for the loop C , the expectation value of such loop variables can be connected to physical observables. For instance, for the so-called Wilson loop, we choose a rectangular loop with size r in one spatial direction and the extension t in the Euclidean time direction (see figure 14, left panel). In the limit of large t , the Wilson loop expectation value is related to the potential $V(r)$ between a static quark and a static anti-quark which are separated by the distance r , i.e.,

$$\langle W[C] \rangle \propto \exp\{-V(r) t\}, \quad (179)$$

In the particular case that the potential is linearly rising, $V(r) = \sigma r$ with **string tension** σ , one observes that the Wilson loop expectation value exponentially decreases with the area A enclosed by the loop C . Since a linearly rising quark anti-quark potential implies confinement (see discussion below), this **area law** (due to Wilson) is a litmus test for quark confinement.

Furthermore, one can calculate the correlation function $L(t_x - t_y, \vec{x} - \vec{y})$ of two loops centred at x and y , respectively (see figure 14), right panel). Here, information is transported from point x to y by gauge invariant states $|ph\rangle$. The shape of a particular loop determines its behaviour under the symmetry transformations of the underlying lattice. These symmetry transformations correspond to rotations in the continuum limit. Therefore, it is possible to select the spin quantum number of the state $|ph\rangle$ by adjusting the shape of the loop. For large distances $\Delta = t_x - t_y$, the correlation function exponentially decreases, i.e.,

$$\sum_{\vec{u}} L(t_x - t_y, \vec{u} = \vec{x} - \vec{y}) \propto \exp\{-ma \Delta\}. \quad (180)$$

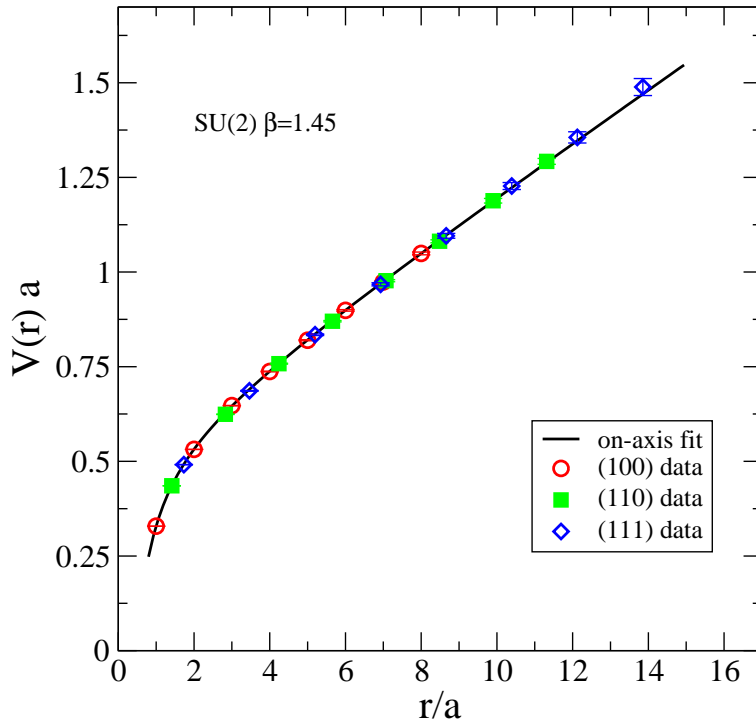


Figure 15: The static quark anti-quark potential as obtained from pure SU(2) lattice gauge theory. Plot from [16].

Hence, the calculation of loop correlation functions provides access to the so-called **screening masses** m of physical particles. In the purely gluonic theory, the only gauge invariant states are the glue balls, while in full QCD also hadronic states contribute to the correlation functions.

5.7 The continuum limit

For definiteness, I confine myself to the case of pure (i.e. no quarks) SU(2) gauge theory. The generalisation of the findings of the present section to $SU(N_c)$ is straightforward. The task is now to find the critical limit of the lattice Yang-Mills theory.

There is a lesson to learn from continuum Yang-Mills theory. In order to renormalise the continuum theory, one absorbs a logarithmic divergence into the bare gauge coupling. A detailed calculation yields

$$\frac{1}{g^2(\Lambda)} = \frac{11}{24\pi^2} \ln \frac{\Lambda^2}{\mu^2} + \text{finite} , \quad (181)$$

where Λ is the UV cutoff and where μ is an arbitrary renormalisation point. The coefficient in front of the logarithmic term is the quantity of interest and can be obtained by evaluating a bunch of one-loop Feynman diagrams. Eq.(181) shows that in the critical limit $\Lambda \rightarrow$

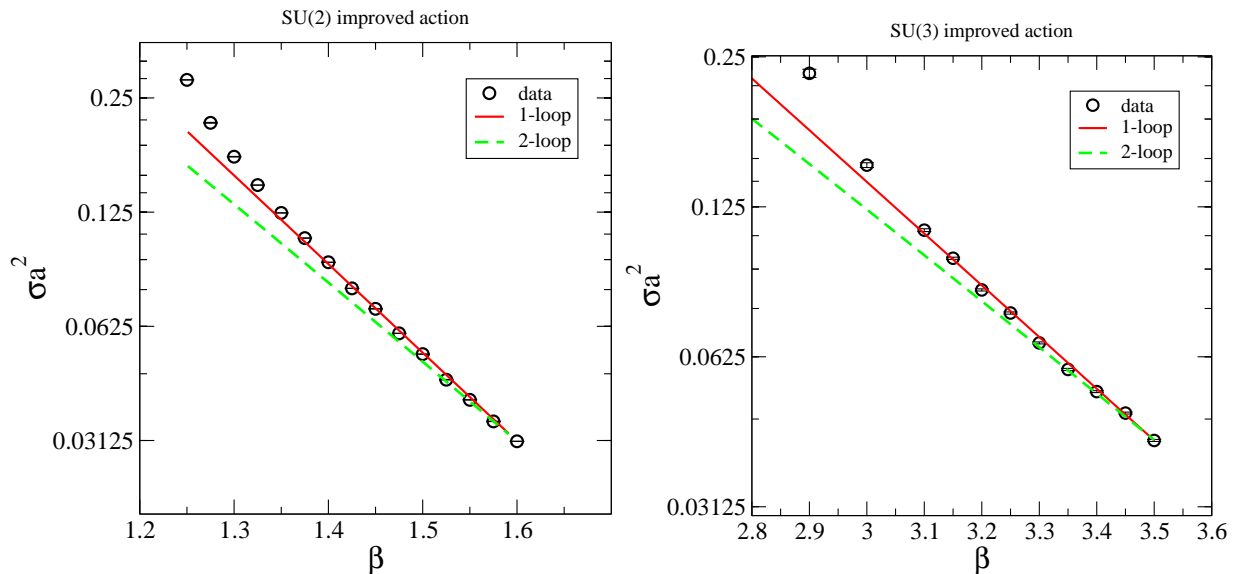


Figure 16: Approaching the continuum limit of SU(2) (left) and SU(3) (right) lattice gauge theory (improved action from [16]).

∞ the bare coupling vanishes. This is one manifestation of the celebrated property of **asymptotic freedom**. Switching from the continuum to the lattice formulation we identify $\Lambda = \pi/a$ and use $\beta = 4/g^2$ to straightforwardly derive

$$a^2(\beta) = \text{const.} \exp\left\{-\frac{6\pi^2}{11}\beta\right\}. \quad (182)$$

Due to asymptotic freedom, we expect that the critical limit is approached when $\beta \rightarrow \infty$. The perturbative relation between a and β in (182) is called *asymptotic scaling*.

Modern computer simulations use a more complicated “kinetic” term for the gluon fields. One example of such an **improved action** is given by

$$S = \beta \sum_{\mu > \nu, x} \left[\kappa_1 \bar{P}_{\mu\nu}(x) + \kappa_2 \bar{P}_{\mu\nu}^{(2)}(x) \right]. \quad (183)$$

where $\bar{P}_{\mu\nu}^{(2)}(x)$ is the 2×2 Wilson loop. Imposing the constraint

$$\kappa_1 + 16 \kappa_2 = 1, \quad (184)$$

ensures that the familiar relation between β and the bare gauge coupling g , $\beta = 2N_c/g^2$, is maintained. The residual freedom of choosing κ_1 and κ_2 can be used to obtain a rather good agreement with asymptotic scaling on rather coarse lattices.

In order to search for the critical limit with the help of numerical simulations, we calculate a physical quantity, e.g. the string tension σ in units of the lattice spacing as a function

of the only parameter β . This is done by calculating the static quark anti-quark potential $V(r)$ as a function of the quark anti-quark distance $r = na$. The outcome in units of the lattice spacing is shown in figure 15. By fitting the numerical data to

$$V(r)a = v_0 - \frac{\alpha}{n} + \sigma a^2 n ,$$

we find the string tension in units of the lattice spacing, σa^2 , for each value of β . The outcome of this calculation is shown in figure 16. One indeed observes that the c-number σa^2 exponentially decreases for large values of β in agreement with the prediction (182) of continuum Yang-Mills theory. The quantum field theoretical limit of the classical lattice model is obtained by interpreting the correlation length, i.e., the string tension σ in the present example, as a fixed physical quantity, and reinterpreting the β dependence of the numerical data for σa^2 as the β dependence of the lattice spacing.

Let us assume we have obtained a glue ball mass m in lattice units, i.e., we know ma as a function of β . If the mass m is a physical observable, one must recover from the data the characteristic dependence $a(\beta)$ (see (182)) for sufficiently large β values. Hence, the ratio of the two dimensionless numbers $m^2 a^2 / \sigma a^2$ approaches a constant for β close to the critical point (see figure 16, right panel). Extrapolating the data to the continuum limit $a \rightarrow 0$, i.e., $\beta \rightarrow \infty$, one determines the physical mass m in units of another physical scale, i.e., $\sqrt{\sigma}$. Finally, let us count the number of parameters. The only parameter of the classical lattice model is β , but β is no longer at our disposal in the quantum field theory limit (which implies $\beta \rightarrow \infty$). However, the physical value of the correlation length (or $\sqrt{\sigma}$ in the present example) takes over the role of a free parameter. The replacement of a dimensionless parameter by a mass scale in the continuum limit is a feature of many quantum field theories and is called **dimensional transmutation**. On the lattice every mass scale is obtained in units of the string tension, $\sqrt{\sigma} = 440 \text{ MeV}$ is used to assign the familiar units of QCD to observables. For 32 lattice points in any space-time direction, we then find:

β (input)	1.250	1.400	1.500	1.600
σa^2 (calculated)	0.279(2)	0.0922(7)	0.0528(3)	0.0311(2)
$L = Na$	7.7 fm	4.4 fm	3.3 fm	2.6 fm
$\Lambda = \pi/a$	2.6 GeV	4.6 GeV	6.0 GeV	7.8 GeV

For a fixed number of lattice points, we note that we cannot make β arbitrarily small since the physical volume becomes too small. Small values of β result in large volumes, but we cannot make β too small in order to have a reasonably large UV cutoff. Thus, for a fixed number of points, there is a small window of β values which are appropriate for a study of QCD particle properties. This window is sometimes called the *scaling window*.

Acknowledgements: I thank Tom Heinzl and Martin Lavelle for a careful reading of the manuscript and helpful comments.

References

- [1] P. Gopikrishnan, V. Plerou¹, L. A. Nunes Amaral, M. Meyer, and H. E. Stanley, *Scaling of the distribution of fluctuations of financial market indices*, Phys. Rev. **E60**, 5305 (1999).
- [2] Michel Le Bellac, *Quantum and Statistical Field Theory*, Clarendon Press, Oxford.
- [3] H. A. Kramers and G. H. Wannier, Phys. Rev. **60**, 252 (1941).
- [4] C. N. Yang, *The spontaneous magnetization of a two-dimensional Ising model*, Phys. Rev. **85**, 808 (1952).
- [5] C. M. Fortuin and P. W. Kasteleyn, *On the Random cluster model. 1. Introduction and relation to other model*, Physica **57**, 536 (1972).
- [6] R. H. Swendsen and J. S. Wang, *Nonuniversal critical dynamics in Monte Carlo simulations*, Phys. Rev. Lett. **58**, 86 (1987).
- [7] U. Wolff, *Collective Monte Carlo Updating for Spin Systems*, Phys. Rev. Lett. **62**, 361 (1989).
- [8] Wolfhard Janke, *Nonlocal Monte Carlo Algorithms for Statistical Physics Applications*, Mathematics and Computers in Simulations **47**, 329 (1998).
- [9] K. G. Wilson, Phys. Rev. D **10**, 2445 (1974).
- [10] see e.g. D. B. Kaplan, *A Method for simulating chiral fermions on the lattice*, Phys. Lett. B **288**, 342 (1992), [arXiv:hep-lat/9206013].
- [11] P. H. Ginsparg and K. G. Wilson, *A Remnant Of Chiral Symmetry On The Lattice*, Phys. Rev. D **25**, 2649 (1982).
- [12] R. Narayanan and H. Neuberger, *A Construction of lattice chiral gauge theories*, Nucl. Phys. B **443**, 305 (1995) [arXiv:hep-th/9411108].
- [13] H. Neuberger, *A practical implementation of the overlap-Dirac operator*, Phys. Rev. Lett. **81**, 4060 (1998) [arXiv:hep-lat/9806025].
- [14] R. G. Edwards, U. M. Heller and R. Narayanan, *A study of chiral symmetry in quenched QCD using the overlap-Dirac operator*, Phys. Rev. D **59**, 094510 (1999) [arXiv:hep-lat/9811030].

- [15] F. D. Bonnet, P. O. Bowman, D. B. Leinweber, A. G. Williams and J. b. Zhang [CSSM Lattice collaboration], *Overlap quark propagator in Landau gauge*, Phys. Rev. D **65**, 114503 (2002) [arXiv:hep-lat/0202003].
- [16] K. Langfeld, *Improved actions and asymptotic scaling in lattice Yang-Mills theory*, Phys. Rev. D **76**, 094502 (2007) [arXiv:0704.2635 [hep-lat]].